



HAL
open science

Non-Invasive On-Site XRF and Raman Classification and Dating of Ancient Ceramics: Application to 18th and 19th Century Meissen Porcelain (Saxony) and Comparison with Chinese Porcelain

Philippe Colomban, Gulsu Simsek Franci, Mareike Gerken, Michele Gironda,
Viviane Mesqui

► **To cite this version:**

Philippe Colomban, Gulsu Simsek Franci, Mareike Gerken, Michele Gironda, Viviane Mesqui. Non-Invasive On-Site XRF and Raman Classification and Dating of Ancient Ceramics: Application to 18th and 19th Century Meissen Porcelain (Saxony) and Comparison with Chinese Porcelain. *Ceramics*, 2023, 6 (4), pp.2178-2212. 10.3390/ceramics6040134 . hal-04283366

HAL Id: hal-04283366

<https://hal.science/hal-04283366>

Submitted on 10 Mar 2024

HAL is a multi-disciplinary open access archive for the deposit and dissemination of scientific research documents, whether they are published or not. The documents may come from teaching and research institutions in France or abroad, or from public or private research centers.

L'archive ouverte pluridisciplinaire **HAL**, est destinée au dépôt et à la diffusion de documents scientifiques de niveau recherche, publiés ou non, émanant des établissements d'enseignement et de recherche français ou étrangers, des laboratoires publics ou privés.



Distributed under a Creative Commons Attribution - NoDerivatives 4.0 International License

Article

Non-Invasive On-Site XRF and Raman Classification and Dating of Ancient Ceramics: Application to 18th and 19th Century Meissen Porcelain (Saxony) and Comparison with Chinese Porcelain

Philippe Colomban ^{1,*}, Gulsu Simsek Franci ², Mareike Gerken ³, Michele Gironda ³ and Viviane Mesqui ⁴

¹ MONARIS UMR8233, Campus Pierre-et-Marie Curie, Sorbonne Université, CNRS, 4 Place Jussieu, 75005 Paris, France

² Koç University Surface Science and Technology Center (KUYTAM), Koç University, Rumelifeneri Yolu, Sariyer, Istanbul 34450, Türkiye; gusimsek@ku.edu.tr

³ Bruker Nano Analytics, Am Studio 2D, 12489 Berlin, Germany; mareike.gerken@bruker.com (M.G.); michele.gironda@bruker.com (M.G.)

⁴ Cité de la Céramique, Grande Rue, 92310 Sèvres, France; viviane.mesqui@sevresciteceramique.fr

* Correspondence: philippe.colomban@sorbonne-universite.fr

Abstract: The authentication and dating of rare ceramics is generally carried out using subjective criteria, mainly based on visual interpretation. However, the scientific study and evaluation of the materials used could contribute objectively. The analytical data relating to the major and minor elements of the coloring agents of the decoration or the base marks, and the characteristics of the raw materials (related to geology and ore processing), can be obtained on the conservation site non-invasively using a pXRF instrument and the phases formed may be identified using Raman microspectroscopy. This approach is applied to 28 objects assigned to the production of the Meissen Factory, from the collection of the Musée National de Céramique, Cité de la Céramique, Sèvres. They have polychromic or blue-and-white decorations and are supposed to have been produced in the 18th and 19th centuries. Some have a production date that has been perfectly established, others may have been produced using an earlier mold, or even have been decorated on an unknown date different from that of the firing of the biscuit. The combination of several classification criteria concerning the type of glaze, previously identified in the study of French and Chinese 17th and 18th centuries productions, i.e., the elements associated with cobalt present in the mark or the blue decoration and the relative levels of impurities of the glaze matrix, both characteristic of the raw materials and giving a strong XRF signal, leads to the identification of groups of homogeneous objects (respectively, counting seven, three, two and two objects for which at least four out of five criteria are identical); the other objects present too many differences to be considered as having been produced with the same raw materials. The first group brings together almost all the objects with a reliable pedigree made before ~1750, but includes two objects with decoration types closer to those of the 1800s. The comparison of the pXRF signals confirms the possibility of identifying the use of European ingredients for the production of painted enamels in the Qing dynasty.

Keywords: porcelain; Meissen; base mark; blue; polychrome; date; cobalt; glaze; raw materials; impurities



Citation: Colomban, P.; Simsek Franci, G.; Gerken, M.; Gironda, M.; Mesqui, V. Non-Invasive On-Site XRF and Raman Classification and Dating of Ancient Ceramics: Application to 18th and 19th Century Meissen Porcelain (Saxony) and Comparison with Chinese Porcelain. *Ceramics* **2023**, *6*, 2178–2212. <https://doi.org/10.3390/ceramics6040134>

Academic Editor: Gilbert Fantozzi

Received: 1 October 2023

Revised: 26 October 2023

Accepted: 9 November 2023

Published: 12 November 2023



Copyright: © 2023 by the authors. Licensee MDPI, Basel, Switzerland. This article is an open access article distributed under the terms and conditions of the Creative Commons Attribution (CC BY) license (<https://creativecommons.org/licenses/by/4.0/>).

1. Introduction

After poorly documented attempts to prepare porcelain by E.W. von Tschirnhaus and J.F. Böttger in Dresden, the Meissen Porcelain Factory was founded in 1710, a few miles from Dresden, under the auspices of Augustus the Strong, Prince Elector of Saxony and King of Poland [1,2]. An almost exhaustive study of regional raw materials was carried out by the two arcanists and, after the discovery of iron-rich kaolin allowing the production of *boccarro* (a red porcelain) [1–7], white clays and iron-free kaolin were discovered in different

places of Saxony, allowing the first production of a mullite-based porcelain in Europe [3–5]. Indeed, the porcelain called soft-paste, that was produced in France at the end of the 17th century in the Rouen and Paris areas, was a very siliceous paste in which quartz grains were bound with a glassy phase, in a rather similar way to Iznik fritware [8–12], different from Chinese porcelain based on a mineralogical point of view. The rare Medici ‘porcelains’, produced over a decade in the 16th century in Florence, have a hybrid character, halfway between soft- and hard-paste porcelain [13]. The Meissen factory plays a very important role in European porcelain history. Then, the number of porcelain factories in Europe increased from less than five active in 1730 to more than fifty in 1780 [3,4,9] (Figure 1). The period of activity of certain factories was reduced to a few years.

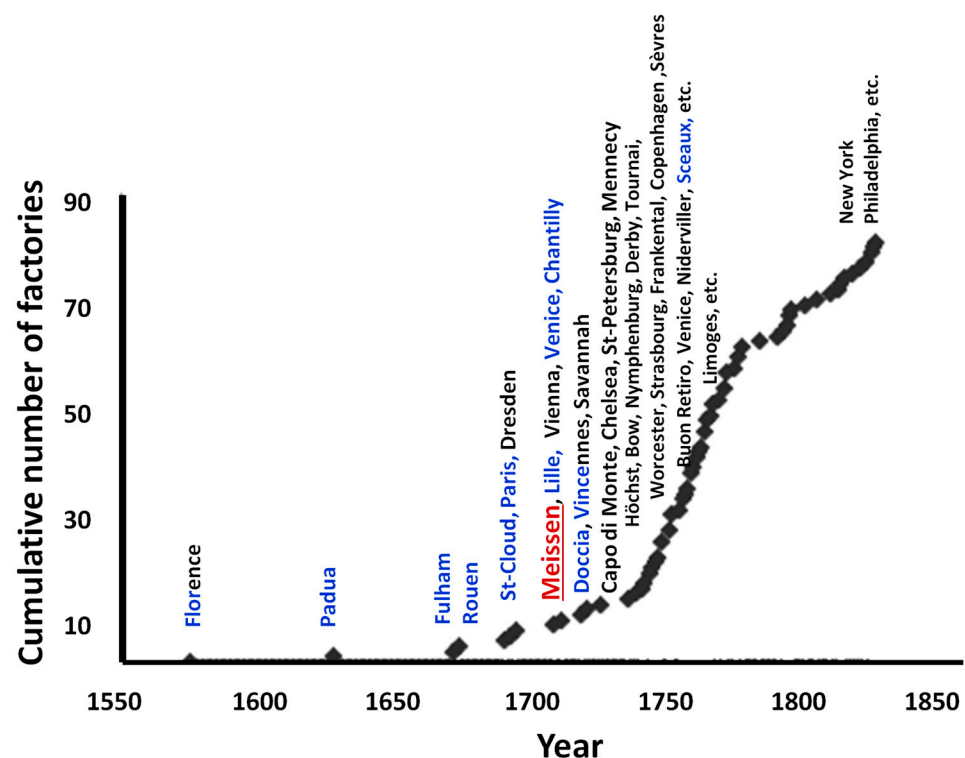


Figure 1. Cumulative number of factories established in Western countries up to 1826. In blue, the production of soft-paste; in black, the production of hard-paste (phosphatic English pastes are included in this class).

At the same time, Chinese export production to Europe developed with, for example, the multiplication of the number of French ships trading with China from a few per decade in the beginning of the 18th century to nearly 50 in the decade of 1770 [14], and with trade via British and Dutch ships becoming multiplied by almost ten times in the second half of the 18th century. This followed a search for information on Chinese know-how encouraged by the authorities as evidenced by the letters of Père d’Entrecolles (also called Dentrecolles) in 1712 and 1722 [15] or the correspondence of French Minister Henri Bertin from ca. 1753 to 1780 [16]. If this quest for know-how, led by Europeans, on producing the best porcelains with the whiteness and blue-and-white decoration of Chinese (and Japanese) models is well known and documented (e.g., [3,4,15,16]), it was only recently that the opposite quest of the Chinese authorities and producers for European know-how in polychrome enameling has been discovered in studying historical reports and began to be studied by collecting information kept in the artifacts [17–27]. Canton (Guangzhou) became a center for the enameling of export porcelain and metalware designed on European models and decorated largely with ingredients and recipes imported from Europe, while the imperial enameling workshop at *Beitang* (The French Church district close to the Forbidden Imperial City)

worked for the court under the guidance of the Jesuits, who were mainly French, but also German and Italian [24–27]. The first analytical studies show connections between the techniques and ingredients used in France [25,26], but the presence of a German Jesuit at the head of the glass workshop (also located at *Beitang*, Beijing) suggests a possible connection with Meissen, likely the leading porcelain factory in terms of decoration and polychrome during the 18th century (Figure 1). This is why the study of Meissen productions with the same procedures as those used for French [9,10,13] and Chinese [22–26] productions was undertaken and is reported here.

Böttger produced the first red porcelain (*boccaro* ware) and then white porcelain [1–7], but a blue pigment, lapis lazuli grains, which is easily detected using Raman microspectroscopy [5], was added by J.F. Böttger to whiten the glaze, which was only opacified by microbubbles. Blue decoration appeared in 1719 and is attributed to David Köhler [1,28]. The first flux used by J.F. Böttger, alabaster (gypsum, calcium sulphate), was replaced after ca. 1730 by feldspar (alkali/earth–alkali aluminosilicate) according to the recipes of Höroldt [1,28]. The analysis of a few shards and broken objects with polychrome decoration by Domoney et al. [29] provided details on the productions between 1725 and 1763 and confirmed the change in composition of the glaze after the Böttger period, from a calcium-based to potassium-based flux. There is evidence of variability in the lead content of the overglaze: 15 to 70 wt% PbO for the blues, ~25–27 wt% for the purples and 33 to 75 wt% PbO for the yellows [28,29]. It is not clear if this variability corresponds to different recipes or if the results of the measurements are distorted by the contribution of the substrate (glaze, body) due to the multilayer nature of the decoration. Arsenic oxide (0.2 to 1 wt%) is detected in the blues, sometimes with traces of barium [28,29]. Tin oxide is observed in the enamels, from 0.5 to 10 wt% for certain purples. The study by Klisinska Kopacz et al. [28] of six figurines corresponding to the initial models of J.J. Kandler from around 1750 shows that a significant rate of zinc oxide characterizes the productions of the 19th century.

We present here the portable X-ray Fluorescence (pXRF) and μ Raman spectroscopy study, carried out in the reserves of the Cité de la Céramique in Sèvres, of 24 objects with polychrome decoration or, more rarely, dichromatic blue-and-white decoration, plus four artifacts only analyzed using Raman microspectroscopy. The objectives are multiple: (i) to evaluate the usefulness of non-invasive measurements for the precise dating and documenting of enameling techniques by focusing on the characterization of decorations and base marks using blue—this color using a rare and geologically peculiar element, cobalt [30]—and gold for gilding or using Au⁰ nanoparticles to obtain a purple to red color, and on impurities characteristic of the raw materials, namely yttrium, rubidium and strontium; (ii) to use the results obtained to discuss whether the transfer of enameling technology carried out under the auspices of the Jesuits to the Qing Court is to be linked to the know-how of the Meissen or Parisian factories. These analytical procedures are those previously developed in the analysis of painted enamels and base marks of 18th century French and Chinese porcelains [22–25]. In fact, the intrinsic heterogeneity of the complex enameled decorations, added to the obligation to carry out the analysis from the surface, leads not only to trying to determine a composition whose accuracy is distorted by the variation in the volume of material probed by XRF as a function of the considered element, on a thickness from a few microns for the light elements (K, Si, . . .) to several mm for the heavy elements (Pb, Sn, Ba, . . .), but to compare the intensity of the signal of characteristic elements in ternary diagrams or in a hierarchical classification [24,25,31]. This procedure has proved its effectiveness [23–26].

2. Objects and Methods

2.1. Objects

Table 1 presents the objects and their marks as well as the dates of the supposed date of manufacture in the museum's database [32]. The date of entry into the collections and the dimensions of the objects are given in the Supplementary Materials (Table S1). The production date is subject to discussion, except for certain objects either dated at the

Meissen manufactory on the body or having a fully documented history. The objects are presented in an order depending on their supposed date of production (assignment made by curators in the 1960s and noted in the museum's internal database; of course, some of these assignments need to be reconsidered). Certain objects entered the collection in 1837 through an exchange between the museum established by Alexandre Brongniart at Sèvres as a reference collection for the French National (Royal/Imperial) Factory of ceramics and its counterpart in Meissen (serie MNC 2274.x) [33], particularly of artifacts that belonged to Augustus the Strong (MNC 2274.20). Some objects were manufactured in honor of specific events (for example, as a gift to Marie Leszcynska or a wedding present for the Dauphin of France and M.-J. of Saxony) [34]. More characteristics are given in Table S1 (dimensions, etc.).

Almost all the artifacts bear the blue mark of two crossed swords on the foot, affixed to the body (see Table 1). This mark is often covered by the glaze. A few specific marks differ: a square imitating a Chinese character (chocolate pot MNC 14229.1), the inscription "Meissen 7 August 1726" (bowl MNC 2274.2/2274.9) and marks engraved with a lapidary (e.g., W, butter cup MNC 2274.20) or painted in black (e.g., K.H.C., Louis XV figure MNC 23181) specific to pieces that belonged to the collection of Augustus the Strong [35]. Only two marks appear brown (Imari-style dish MCSR XXXXV and tureen MCSR LXXIX). The positioning constraints of the object that were incompatible with the focusing of the X-ray beam (pXRF) or the laser beam (μ Raman) prevented the analysis of certain marks.

Table 1. View of the studied artifacts and their marks. The expected date of production is given (MCSR-Musées Nationaux Récupération [36]). Red spots help to optimize the focus of the X-ray beam. Perfect focus is achieved when both spots superimpose (photos P. Colombar). More details (dimensions, date of acquisition, etc.) are given in Table S1 (Supplementary Materials).







Inventory Number (Type)	Period (from Ancient Assignments)	View	Mark	XRF Analyzed Spot
MNC 2274.38 (Figure)	1709–1730			
MNC 469.11.1 (tea cup)	ca. 1720–1725			Not pXRF analyzed
MNC 8160.2 (dish)	ca. 1720		Not pXRF analysed	Not pXRF analyzed

Table 1. Cont.

Inventory Number (Type)	Period (from Ancient Assignments)	View	Mark	XRF Analyzed Spot
MNC 2274.9 (2274.2) (bowl)	1726 (mark)			
MCSR XXXXV (Imari-style dish)	ca. 1730			
MCSR LXXIX (tureen)	ca. 1730			
MNC 19014 (coffee cup with coats of arms of France and Poland)	1737 Gift from August III to Marie Leszcynska			
MCSR LVII.1 (coffee cup with Watteau-like décor)	ca. 1745			Not pXRF analyzed
MNC 8322	ca. 1740–1760			
MNC 23181 (Louis XV figure)	c.a. 1746 (wedding of France Dauphin and M.-J. de Saxe)			No blue mark

Table 1. Cont.

Inventory Number (Type)	Period (from Ancient Assignments)	View	Mark	XRF Analyzed Spot
MNC 11205 (Bacchus and bacchante group)	Käendler period ca. 1760			Not pXRF analyzed
MNC 2274.20 (butter cup)	18th c. c.a. 1730			
MNC 19032.2 (mustard cup)	18th c.			
MNC 14229.1 (chocolate pot)	18th c.			
MNC 11213.2 (coffee cup)	18th c.			
MNC 14234 (orange cup)	18th c.?			
MNC 11051.2 (boy figurine)	18th c.?			

Table 1. Cont.


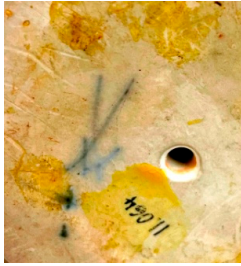



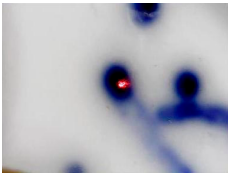

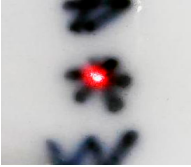

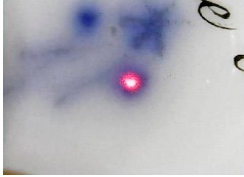




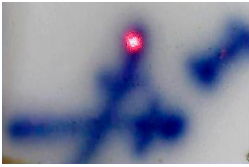

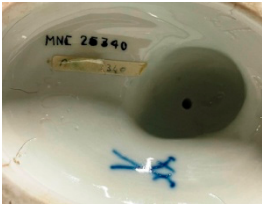


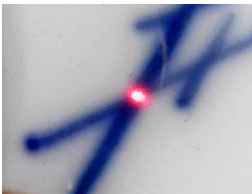


Inventory Number (Type)	Period (from Ancient Assignments)	View	Mark	XRF Analyzed Spot
MNC 11064 (Group of three child geometers and astronomers)	18th c.?			
MNC 19944 (singing angel)	18th c.		No mark	
MNC 9638 (bowl)	18th c.		Not pXRF analyzed	Not pXRF analyzed
MNC 14201 (tea pot)	18th c.			
MNC 23298.1 (cup for Turkish market)	ca. 1774–1814			
MNC 469.9.1 (coffee cup with painting copy)	ca. 1774–1814 (Marcolini period)			
MNC 886.4.1 (coffee cup)	end of 18th c. to beginning of 19th c.			

Table 1. Cont.

Inventory Number (Type)	Period (from Ancient Assignments)	View	Mark	XRF Analyzed Spot
MNC 469.5.1 (coffee cup)	19th c.?			
MNC 25340 (figure)	19th c.			
MNC 886.3 (dish)	1825			
MNC 2247.10 (dish)	19th c.?			

2.2. pXRF Analyses

X-ray Fluorescence analysis was performed on-site using a portable ELIO instrument (ELIO, Bruker, Berlin, Germany) as described in previous studies [23–25]. The set-up includes a miniature X-ray tube system with a Rh anode (max voltage of 50 kV, max current of 0.2 mA and a 1 mm collimator) and a large area Silicon Drift Detector (SDD, 50 mm² active area) (ELIO, Bruker, Berlin, Germany) with an energy resolution of <140 eV for Mn K α . Depending on the object, the measurement is carried out by positioning the instrument on the top or on the side. A perfect perpendicularity to the area being measured is needed. When the shape of the object does not allow a perfect positioning, scattering contribution between ~19 and 22 keV becomes important. Focusing is controlled by the red laser (see photos in Table 1). Measurements were carried out using the point mode with an acquisition time of 120 s, using a tube voltage of 50 kV and a current of 80 μ A. No filter was used between the X-ray tube and the sample. The signal-to-noise ratio (SNR) of the spectral signals was optimized with the set-up parameters described above. The analysis depth, defined as the thickness of the top layer from which 90% of the fluorescence originates (which depends on the photon energy, type of material (atom number) and material density), was calculated using Beer–Lambert law [37]: the probed thickness is estimated to be close to 6 μ m at Si K α , 170 μ m at Cu K α , 300 μ m at Au L α and 3 mm at Sn

$K\alpha$. Due to the resolution of the energy-dispersive detector and the close location of the Fe $K\beta$ lines (7.0593 keV) and the Co $K\alpha$ lines (6.9309 keV), the two peaks are overlapping.

After recording the raw data with ELIO, the spectra files in Bruker spx format are opened using the Artax 7.4.0.0 (Bruker, AXS GmbH, Berlin, Germany) software. The major (e.g., K, Ca), minor (e.g., Fe, Ti, Co) and trace elements (e.g., Ag, Bi, As and U) are added in the periodic table. For the correction, escape and background options are selected in the Method Editor and 10 cycles of iteration were selected, starting from 0.5 keV to 45 keV. The deconvolution method, Bayes, was applied for the exporting of results. The net area under each peak was calculated at the characteristic energy of each element selected in the periodic table and the counts of the major, minor and trace elements were plotted in the ternary scattering plots drawn using the software Statistica 13.5.0.17 (TIBCO Software Inc., Palo Alto, CA, USA). For a comparison of these data with the older measurements, especially those carried out with Bruker instruments but using its different portable models, a normalization procedure can be applied by taking the ratio of the major (K, Ca), minor (Mn, Ni, Fe, Cu, As) and trace elements (Ag, As, Bi, U, Zr, Y, Sr, Rb) with the number of XRF photons derived from the elastic peak of the X-ray tube of rhodium. We also normalized the data to the major element found in the matrix that we analyzed; for instance, Si in the enamel, in addition to the calculation of the ratios of the net number of XRF photons of the elements (K, Mn, As, Ni, Fe, Cu, Zn, Bi, Ag) versus cobalt (coloring element for blue).

For the interpretation of the results using a statistical approach, a hierarchical Euclidian clustering diagram was drawn by using the data obtained from the XRF photons of Pb, K, Mn and As with the software Statistica (Statsoft-TIBCO Inc., Palo Alto, CA, USA).

Corrected XRF spectra are presented in Figure S1 (Supplementary Materials).

2.3. Raman Microspectroscopy

Raman analyses were carried out in the storage room of the Sèvres museum with a mobile HE532 Raman set-up (HORIBA Scientific Jobin-Yvon, Longjumeau, France) as extensively described in reference [22]. For each colored area in the objects concerned, at least three Raman spectra were recorded to check the representativeness of the collected data on a statistical basis. The reliability of the Raman spectrum starts above 80 cm^{-1} but a flat spectral background is only obtained over 500 cm^{-1} . A $50\times$ (17 mm long working distance, Nikon France SAS, Champigny-sur-Marne, France) objective was used (surface spot waist $\sim 2\text{--}4\text{ }\mu\text{m}$; in-depth $< 5\text{--}10\text{ }\mu\text{m}$, the values varying with the color) by positioning it perpendicular to the sample surface, which allowed for the recording of spectra which are not affected or only minimally affected by the sub-layers and/or the silicate matrix if the grains are bigger than $\sim 5\text{ }\mu\text{m}$. Obviously, the power of illumination at the sample should be minimal ($\sim < 1\text{ mW}$) for dark colored areas due to the absorption of light, although up to 10 mW is required for the examination of light-colored or colorless areas of the enamels and more than $\sim 20\text{ mW}$ for paste.

As-recorded Raman spectra are presented in Figure S1 (Supplementary Materials).

3. Results

3.1. Information on the Elemental Composition

To obtain a sophisticated decoration, the painted enamels (also called overglaze) are applied thinly, a few tens to hundreds of microns in thickness, and a high heterogeneity in the concentration of coloring agents is required at a few millimeter scale [11,30,38]. Due to the intrinsic variation in the volume of material analyzed by pXRF as a function of the energy of characteristic element peaks, and the beam diameter being much larger than the size of the coloring pigments [37], it is not possible to calculate the exact composition of the enamel from measurements made at the surface [23–25]. On the other hand, a comparison of the signals (corrected for the continuous background and the operating conditions, and, if necessary, normalized with respect to the signal of another element) allows for a comparison of the relative content of selected elements of the raw materials with similar composition. Previous studies have shown that a comparison of elements

with similar Z number (i.e., with the XRF peak in a similar energy window and hence similar in-depth penetration) is reliable [12,24,25]. However, the signal of the coloring element(s) and associated elements can be reduced by the contribution of the colorless glassy matrix. Moreover, for example, for the marks, the colored zone can have an inferior thickness and surface than that of the measured zone that increases the contribution of colorless neighboring volume (body and/or glaze). The volume of matter under and over the painted mark will contribute significantly to the XRF signal.

Figure 2 shows the XRF spectra representative of the different categories of glazed decoration. The elements lithium and boron are never detectable by pXRF and sodium cannot be detected in our conditions, where we operated a pXRF without a vacuum pump or He flux. The differentiation between a potassium- (MNC 2274.9) and calcium-based flux glaze (e.g., MNC 469.5.1 pink) and a Pb-rich glaze (MNC 469.5.1) is obvious. Indeed, the detection of lead (MNC 469.5.1) is evident in the energy range below 15 keV. In the case of gilding, despite its low thickness (about 1 μm [38]), the spectrum is dominated by Au-L lines. As with lead, numerous transitions are intense, in particular $L\alpha$, $L\beta$ and $L\gamma$. Note the significant intensity of the peaks of the impurities Rb, Sr, Y and Zr ($K\alpha$ transitions) in comparison with that of the majority element, Si. The pXRF analysis will be particularly effective for these elements because of the poorer effect of attenuation on their high energy lines that can be used to separate ingredients from different geological contexts. Moreover, note that, for the resolution of the instrument, the Fe $K\beta$ and Co $K\alpha$ lines are almost superimposed. It is necessary to consider the relative intensity of Fe $K\alpha/K\beta$ and the width of Fe $K\beta$ line to visually detect cobalt in small quantities. It is the same for the superposition of Pb $L\alpha$ and As $K\alpha$, only As $K\beta$ is visible just below Pb $L\beta$ line [23–25,39,40]. Slight surface pollution on the entire surface of the porcelain during overglaze firing is detectable, as for the MNC 2274.9 bowl, due to the large sensitivity of XRF analysis in the detection of lead.

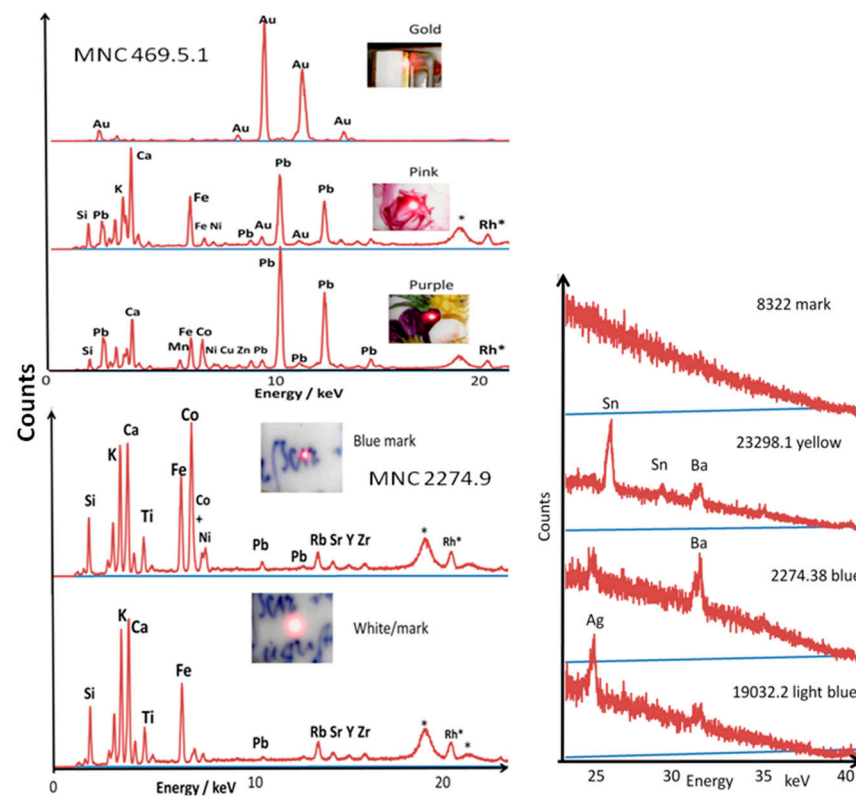


Figure 2. Examples of pXRF spectra showing the main types of signatures (peaks marked with * arise from the instrument) of MNC 469.5.1, 2274.9, MNC 8322, MNC 22298.1, MNC 2274.38 and 19032.2

MNC 19032.2 artifacts. Main elements at the origin of transition peak are given. Visible images of the analyzed spot (~1 mm diameter) are shown. All XRF spectra are presented in Figure S1 (Supplementary Materials).

The 20–40 keV range contains the characteristic peaks of heavy elements like Sn, Ba and Ag (Figure 2).

The Artax processing procedure allows the precise measurement of the areas of the characteristic peaks and their comparison. All of the XRF spectra are given in the Supplementary Materials and the elements identified are listed in Table 2, classified as major or minor/trace elements.

Table 2. Crystalline and amorphous phases (main peak wavenumbers are given in cm^{-1}) and elements identified via visual observation of the Raman and XRF spectra (Naples: Naples yellow; w: wollastonite; cas: cassiterite; ars: lead arsenate; MnO_2 : MnO_2 -rich phase; stret.: stretching mode; X: not identified; Fluo: fluorescence). The main elements associated to cobalt are used to define groups (photos P. Colombari).


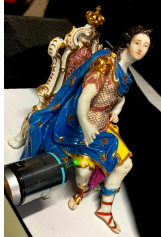
Inventory Number (Type)	Types and Period Assignment (This Work)	View	Raman Analyzed Spots	Phases (SiO_4 Stret. In cm^{-1})	XRF Analyzed Spots	Major Elements (Other than Si)	Other Elements
MNC 2274.20 (butter cup)	[Cu-Zn] _{Co} [Ni] _{Co}		blue glaze	Si-rich (910–1050) Si-rich (910–1050)	blue glaze	K,Ca,Fe K,Ca,Fe	Co,Ti,Ni,As,Rb,Sr,Y,Zr,V Ni,Ti,As,Rb,Sr,Y,Zr,V
MNC 2274.2 (bowl)	[Cu-As-Ni] _{Co} [Ni] _{Co}		green see ref. [5]	Si-rich (1100), cas	green glaze pink gold mark	Pb,Ca,Fe,Cu K,Ca,Fe Pb,Ca,Fe Au K,Ca,Fe	K,Ni,Ti Ti,Ni,Rb,Sr,Y,Zr,Pb Au,Ni,Cu Pb,Fe,Ca,K Co,Ni,Ti,Rb,Sr,Y,Zr,Pb
MNC 19014 (coffee cup with arm coat of France and Poland)	[Cu] _{Co} [Ni] _{Co}		blue green yellow brown orange	mixed (1000), cas Sb-Naples, w Sb-Naples, w Mn oxide hematite	blue glaze purple gold mark	Pb Ca,K,Fe Pb,Ca,Fe Au K,Ca,Fe	Co,As,K,Ca,Fe,Ni Ti,Ni,Rb,Sr,Y,Pb Au,Ni,Rb,Sr Pb,Fe,Ca,U Co,Ni,Rb,Sr,Ti,Pb
MNC 23181 (Louis XV figure)	[Cu] _{Co} [Ni] _{Co}		blue glaze pink yellow	Si-rich (1050) Si-rich (1050–1100) Fluorescence Sb-Naples, w	blue glaze gold pink	Pb,Ca,K K,Ca,Fe Au,Pb Pb,Ca,Fe	Fe,Co,Ni,Sn,Ba Pb,Rb,Sr,Y Ca,Fe,U Au,Rb,Sr,
MNC 19032.2 (mustard cup)	[Cu] _{Co} [Ni] _{Co}		blue yellow green purple red	Cass, ars, (1000) Sb-Naples, X Sb-Naples, X Fluorescence Hematite	dark blue light blue glaze pink purple yellow mark	Pb Pb K,Ca,Fe Pb,Fe Pb,Fe Pb,Fe K,Fe	Co,Fe Co,Fe,As,Ag,Ba Ti,Ni,Rb,Sr Au,Ni,Cu,Zn Au,Ni,Cu,Zn Mn,Ni Ca,Co,Ni,Rb,Sr,Y
MCSR XXXXV (Imari-style dish)	[Cu-As] _{Co} [Ni] _{Co}		dark blue blue green red	Si-rich (1010–1120) Si-rich (1010–1120) Sn-Naples Hematite	blue glaze gold mark (black)	Ca,K,Fe Ca,K,Fe Au, Ca,K,Fe	As,Co,Ni,Cu,Ti Rb,Sr,Y,Zr Fe,Ni Fe,Ni,Rb,Sr,Y,Zr,Pb

Table 2. Cont.










Inventory Number (Type)	Types and Period Assignment (This Work)	View	Raman Analyzed Spots	Phases (SiO ₄ Stret. In cm ⁻¹)	XRF Analyzed Spots	Major Elements (Other than Si)	Other Elements
MNC 14229.1 (chocolate pot)	[Cu-As] _{Co} [Ni] _{Co}		blue	Si-rich (910–1050)	blue glaze mark	K,Ca,Fe K,Ca,Fe K,Ca,Fe	Co,Ti,V,Ni,Rb,Sr,Y,Pb Ti,V,Mn,Rb,Sr,Y,Zr Co,Ti,V,Mn,Rb,Sr,Y,Zr
MNC 8322	[Cu-As] _{Co} [Ni] _{Co}		glaze yellow green orange	Si-rich (1050–1100) Sb-Naples Sb-Naples Hematite	glaze blue pink mark	Ca,K,Fe Pb Pb,Ca,Fe K,Ca,Fe	Ti,Ni,Rb,Sr,Y,Pb Co,Fe,Ca,Ni,As,Ti Au,Ni,Ti Co,Ni,As,Rb,Sr,Y
MNC 14234 (orange cup)	[Cu-As] _{Co} [Ni] _{Co}		blue glaze	Si-rich (1010–1120) Si-rich (1010–1120)	blue glaze mark	Ca,K,Fe Ca,K,Fe Ca,K,Fe	As,Co,Ni,Cu,Rb,Sr,Y Rb,Sr,Ni,Ti Co,Ni,As,Rb,Sr
MNC 469.9.1 (coffee cup with painting copy)	[Cu-As] _{Co} [Ni] _{Co}		blue brown red	Si-rich (1000–1100) Si-rich (1050) hematite	blue glaze gold mark	Co K,Ca,Fe Au K,Ca,Fe	K,Ca,Ti,Fe,Ni,Cu,As Ti,Ni,As,Rb,Sr,Y,Zr Fe,As,Ag,Ba Ti,Co,Ni,Cu,As,Rb,Sr,Y
MNC 886.4.1 (coffee cup)	[Cu-As] _{Co} [Ni] _{Co}		Blue glaze	Si-rich (1000–1050) Si-rich (1050)	blue glaze gold mark	Co K,Ca,Fe Au K,Ca,Fe	K,Ca,Ti,Fe,Ni,Cu,As,Rb Ti,Ni,Rb,Sr,Y,Zr Fe,As Co,Ni,Ti,As,Rb,Sr,Y,Zr
MNC 2274.38 (Figure)	[Cu-As] _{Co} [-] _{Co}		dark blue yellow glaze	Arsenate Sb-Naples Mixed (1060)	blue white pink mark body	Pb,Ca,K Pb,K,Ca K,Fe K,Ca,Fe K,Ca,Fe	Co,As,Zn,Fe,Ni,Ag,Ba Fe,As,Co,Zn,Ni Ca,Au,Ni,Ti,Rb,Sr Co,Ni,Rb,Sr,Cu,Ti Ti,Rb,Sr
MNC 14201 (teapot)	[Cu-Zn] _{Co} [?] _{Co}		blue brown yellow green	Si-rich (1000) Spinel Sn-Naples, cas Sb-Naples	glaze	K,Ca,Fe	Ti,Ni,Pb,Rb,Sr,Y,Zr
MCSR LXXIX (large tureen)	[Zn] _{Co} [-] _{Co}		blue yellow green black	Si-rich Sb-Sn Naples Sb-Sn Naples MnO ₂	blue glaze pink gold mark	Pb K,Ca,Fe Pb,Fe,Ca,K Au K,Ca,Fe	Zn,Co,Fe,Cu,Ca Ti,Ni,Rb,Sr,Y,Pb Au,Zn,Ni,Ti As,Pb,U Co,Ni,Rb,Sr,Y,Pb
MNC 11213.2 (coffee cup)	[Zn] _{Co} [Zn] _{Co}		blue yellow green red	Si-rich (1000–1100) Sb-Sn Naples Sb-Sn Naples, Fluorescence	blue glaze pink purple gold	Zn,Pb K,Ca,Fe Pb,K,Ca,Fe Ca,Zn,Pb Au	Co,Ca,Fe,Ni,Ti Ti,Ni,Rb,Sr,Y,Zr,U Au,Zn,Ti,Rb,Sr,Y,Zr Co,Fe,Ni K,Ca,Fe,U

Table 2. Cont.


Inventory Number (Type)	Types and Period Assignment (This Work)	View	Raman Analyzed Spots	Phases (SiO ₄ Stret. In cm ⁻¹)	XRF Analyzed Spots	Major Elements (Other than Si)	Other Elements
MNC 11051.2 (boy figure)	[Zn] _{Co} [Zn] _{Co}		blue	Si-rich (1000),?	Dark blue light blue glaze mark	Pb,Zn Pb,Zn K,Ca,Pb,Fe Fe,Co,K	Co,Fe Co,Fe,As,Ni,Ti Ni,Cu,Zn,Ti Ca,Ni,Rb,Sr,Pb
MNC 11064 (Group of three child geometers and astronomers)	[Zn] _{Co} [Zn] _{Co}		dark blue light blue orange	Si-rich (1000), ars Si-rich (1000),? Hematite	dark blue light blue glaze gold mark	Pb,Zn Pb,Zn K,Ca,Fe Au Fe,K	Ca,Co,As,Sn,Ba,Ni Ca,Co,As,Sn,Ba,Ni Ti,Ni,Pb,Rb,Sr Ca,Ti,Fe,Ni,Pb,U Ca,Ti,Ni,Pb,Rb,Sr
MNC 11205 (Bacchus and bacchante group)	[Zn] _{Co} [Zn] _{Co}		dark blue blue brown green	? Si-rich (1050) Fluo, Sn-Naples Sn-Naples, spinel?	Blue pink gold	Pb,Zn Ca,Pb,Zn Au	K,Ca,Fe,Co,Ni K,Ni,Cu,Au.,U Ca,Fe,K,Ni,Cu,Pb
MNC 23298.1 (cup for Turkish market)	[Zn] _{Co} [Zn] _{Co}		blue yellow	- Sb Naples	blue glaze yellow pink red mark gold	Zn,Pb K,Ca,Fe Pb Ca,Fe,Pb Pb,Ca Ca,Fe Au	Co,Ca,Ni Ti,Fe,Ni,Pb,Rb,Sr,Y,Zr Ca,Fe,Sn,Ba K,Ca,Ti,Ni,Au,Rb,Sr,Y K,Ti,Fe,Ni,Cu,Au,Rb,Sr Co,K,Ti,Ni,As,Rb,Sr,Y Ca,Fe,Pb,U
MNC 19944 (singing angel)	[Zn] _{Co} [Zn] _{Co}		blue	Si-rich (950–1150), ars	blue glaze gold mark	Pb,Zn K,Ca,Fe Au,Pb,Zn K,Ca,Fe	Ca,Fe,Co,Ni Ti,Ni,Pb,Rb,Sr,Y,Zr Ti,Co,Ni,Rb,Sr,Y,Pb
MNC 469.5.1 (coffee cup)	[Zn] _{Co} [Zn] _{Co}		blue yellow green pink purple red	Si-rich (1000), ars Sb-Naples Sb-Naples Fluorescence Fluorescence Hematite	blue glaze pink purple gold mark	Zn,Pb K,Ca,Fe Ca,Pb,Fe Pb,Ca Au K,Ca,Fe	Co,Pb,Fe,As,Ca,Ni Ti,Ni,Pb,Rb,Sr,Y,Zr K,Ni,Ti,Au,Rb,Sr Ti,Ni,Mn,Cu,Zn,Au Co,Ni,Rb,Sr,Ti

Table 2. Cont.








Inventory Number (Type)	Types and Period Assignment (This Work)	View	Raman Analyzed Spots	Phases (SiO ₄ Stret. In cm ⁻¹)	XRF Analyzed Spots	Major Elements (Other than Si)	Other Elements
MNC 469.11.1 (tea cup)	[Zn] [-]		blue glaze green yellow pink	Si-rich (1050–1100) Si-rich (1100) Sb-Naples ? Fluorescence	blue pink gold	Zn,Co,Pb Pb,Fe,Ca Au	Fe,Ni,Ca Zn,Co,Ni Pb
MNC 886.3	[Zn-As] _{Co} [Ni] _{Co}		glaze blue	Si-rich (1050–1150) Si-rich (1050–1150)	blue glaze mark	K,Ca,Fe K,Ca,Fe K,Ca,Fe	Co,Ti,Ni,Zn,As,Rb,Sr,Y,Zr Ti,Ni,Zn,Rb,Sr,Y,Zr Co,Ti,Ni,Zn,As,Rb,Sr,Y,Zr
MNC 2247.10 dish	[Ag] _{Co} [Ni] _{Co}		blue glaze	Si-rich (1000–1150) Si-rich (1000–1150)	blue glaze mark	Ca K,Ca,Fe K,Ca,Fe	K,Co,Ti,Fe,Ni,Cu,Zn,Rb,Sr,As T,Ni,Rb,Zr,Sr,Y Co,V,Ni,Rb,Zr,Sr,Y,As
MCSR LVII.1 (coffee cup with Watteau-like décor)			glaze black yellow green orange	Si-rich (1100) Spinel Sb-Naples, w Sb-Naples, w Hematite	not studied		
MNC 8160.2 (dish)			blue yellow pink	Si-rich (1000) Sb-Naples, Fluorescence	Not studied		
MNC 25340 (figure)			glaze yellow green light green purple orange black	Si-rich (1100) Sn-Naples, cas Sn-Naples, cas Sn-Naples, cas Fluorescence Hematite spinel	Not studied		
MNC 9638 (bowl)			dark blue yellow grey green pink orange	? Sb-Sn Naples Sb-Sn Naples Sn-Naples Fluorescence Hematite	Not studied		

Figure 3 shows the Raman spectra (as-recorded) representative of the different glazes and overglazes. Similar Raman signatures have been recorded and assigned in previous papers [5,7,9,22–26].

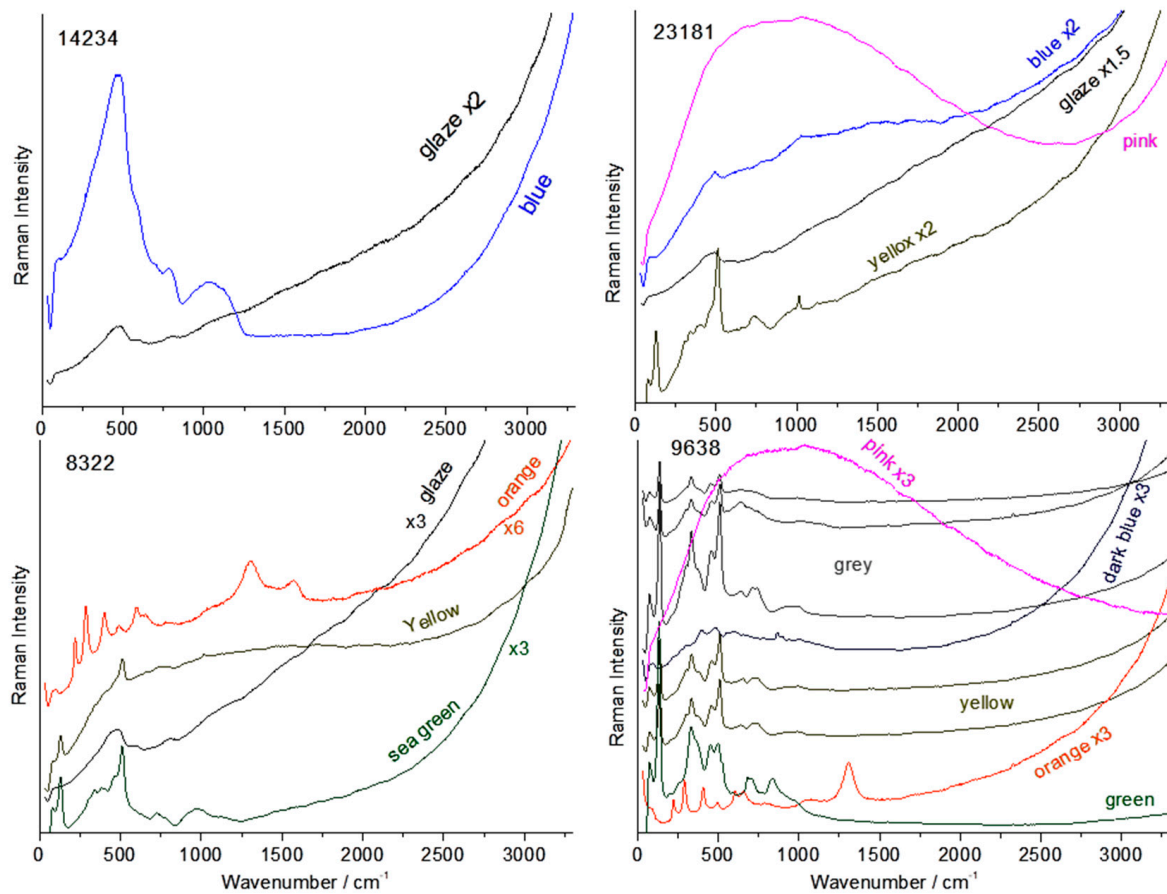


Figure 3. Examples of Raman spectra (recorded from MNC 14234, MNC 8322, MNC 23181 and MNC 9638 artifacts). The color of the analyzed area is given.

The spectrum of the orange cup MNC 14234 corresponds to the colorless glaze and to the same glaze colored blue by cobalt ions. The Raman signature is identical, but the blue color absorbs a large part of the fluorescence that flattens the background, which makes it easier to see the Raman spectrum, which is typical of a potassium–calcium flux porcelain glaze [9] fired at a high temperature; an intense band towards 500 cm^{-1} is characteristic of the deformation modes of the SiO_4 tetrahedron (the vibrational unit of silicates [41,42]) is observed. The band around 1000 cm^{-1} , characteristic of the symmetric stretching A_1 mode of the SiO_4 tetrahedron, has a much weaker intensity. For a lead-rich glaze, the intensity of the SiO_4 stretching mode is the strongest and observed at a lower value, typically 900 cm^{-1} [41,42] (see, e.g., the spectrum of sea-green area in the MNC 8322 artifact or the grey or yellow areas in the MNC 9638 artifact (additional narrow peaks arise from the crystalline pigment(s))). Similar K-Ca-glaze spectra are observed for the MNC 23181 object (colorless and blue glaze). The wavenumbers of the principal component(s) of the stretching band are given in Table 2.

The spectrum of the pink to purple color of the MNC 9638 and MNC 23181 objects shows a characteristic spectrum of the fluorescence linked to the metal nanoparticles at the origin of the color [43]. The other spectra that show a series of well-defined peaks are characteristic of the crystalline phases, which can be identified using the literature [10,44–50] and are dispersed in the vitreous silicate matrix (the SiO_4 tetrahedron modes at ~ 500 and 1000 cm^{-1} are more or less visible). They are hematite for red to orange areas (MNC 8322 and MNC 9638, Figure 3) [7,46] and pyrochlores (called Naples yellow or lead-tin yellow depending on the composition, MNC 23181, MNC 8322 and MNC 9638, Figure 3) for yellow, grey and green areas [45–49]. All of the Raman spectra are given in Figure S1, Supplementary Materials.

3.2. Glaze and Enamel Flux

Ternary diagrams are constructed using the XRF characteristic signal of elements that, in some way, distort the composition diagram; these distortions could be constructed from the contents of these elements, like the replacement of a geographical map by its equivalent, as a result of the time necessary to join the localities via public transport. The data forming clusters in these diagrams would also have formed clusters in a composition diagram. On the other hand, the distances between clusters depend on the elements considered.

We are going to look at the distribution of the intensities of the characteristic signals of the elements leading to the lowering of the melting temperature of enamels (ingredients called fluxes), namely lead, alkaline–earth metals (Ca, Ba) and potassium. Figure 4a compares the relative intensities of the elements making up the flux and detected using pXRF: Pb, Ca and K. We will also discuss the presence of the characteristic barium peak, as visually observed on certain spectra. At the bottom of the Ca-K line are the measurements made on the blue marks (the marks of the Imari-style MCSR XXXXV and tureen MCSR LXXIX are brown) and on the uncolored covers (‘white’) measured close to the mark (see the photographs in Table 1). The painted mark is thin and, consequently, the fluxing elements of the substrate (the paste) and the colorless glaze that cover the mark can be dominant in the probed volume.

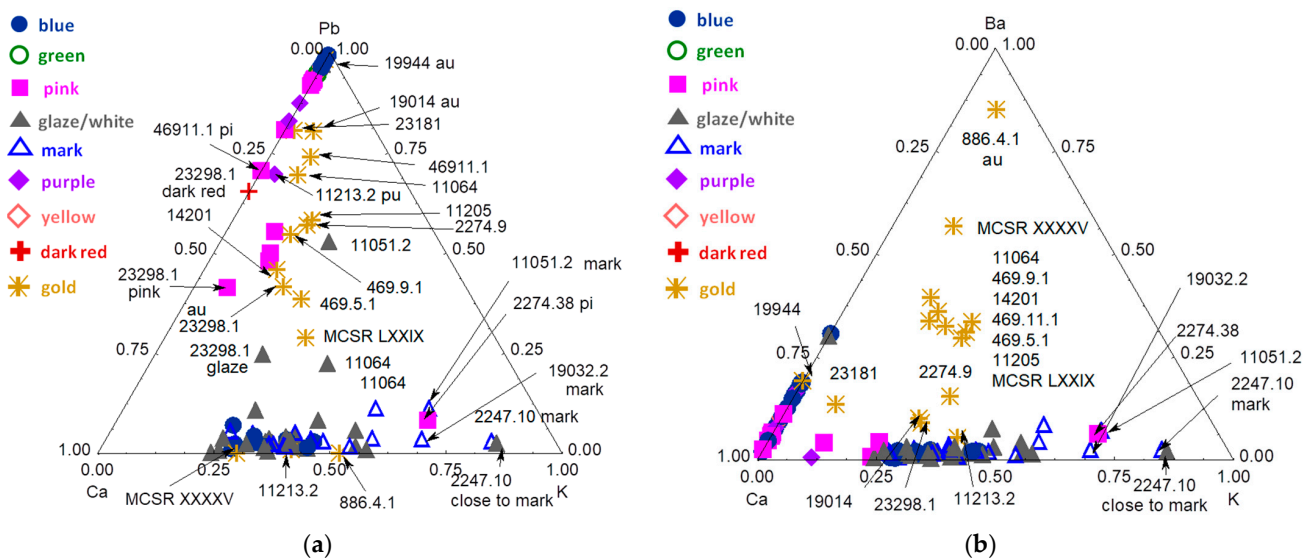


Figure 4. Ternary diagrams of the relative intensities of the signal of the elements constituting fluxes: Pb, Ca, K (a) and Ba, Ca, K (b). The inventory numbers MNCx of the objects and the area analyzed (color, mark, glaze) are indicated (see Table 1).

At the top near the Pb vertex are the lead-based overglazes. The values distributed between the top and bottom values arise from the variable lead contents and/or variable thicknesses; indeed, the large depth contributing to the Pb-L signals implies a contribution from the glaze under the overglaze, or even from the paste, both containing a significant amount of calcium and potassium. The substrate may also contribute to the measurements made on gilded areas. The gold foil is about 1 μm thick [50], in comparison to the in-depth explored by the X-ray beam, which is a few hundreds of μm ; these different values are (roughly) aligned on the line joining the Pb peak to the average value of the Ca/K ratio of the glaze. A few objects appear abnormal out of the group, and we will discuss these later: MNC 11064 light blue; MNC 19032.2 dark blue-very light blue-purple; MNC 469.11.1: blue; MNC 469.5.1: blue; MNC 11051.2: dark blue-light blue; MNC 19944: gold; and MNC 2274.38 (triangle and circle): white-blue. The Ba-Ca-K ternary diagram (Figure 4b) shows the presence of traces of barium associated with gilding, probably coming from the flux added to the gold nanoparticles. Two groups are observed on the ternary scattering plot

of Ba-Ca-K. One is aligned on the Ca-Ba distribution and the other is aligned on the Ca-K axis. The first one corresponds to the analyses of glazes rich in calcium and the second one refers to the analyses of marks painted over a paste richer in potassium. The contribution of the substrate imposes the clustering in this diagram.

The trace elements Y, Rb, Sr and Zr were chosen (Figure 5) because the signals of these traces are intense in XRF and contain much information. Previous works have shown that the contents of these elements separate the Asian raw materials from those imported and used by French porcelain factories [24,39,51] due to the very different geological context (in a simplified way, the old Hercynian mountains and sedimentary basin in Europe, and Himalaya-driven modern orogenesis in Asia [30]).

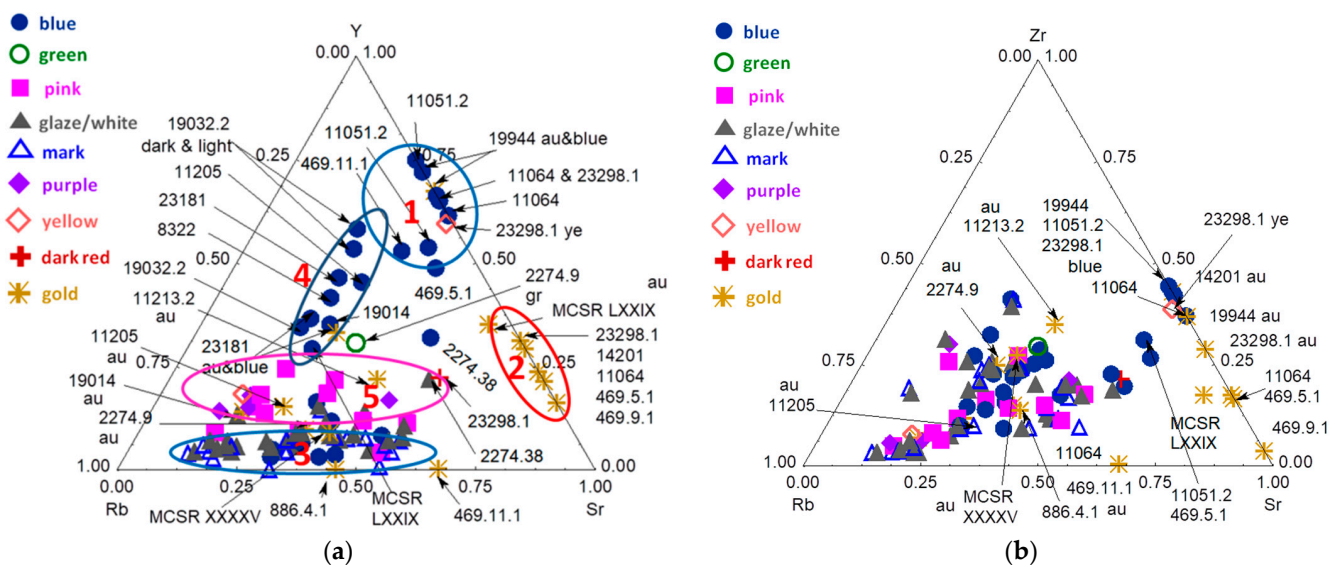


Figure 5. Ternary diagrams of the relative intensities for the elements Y, Rb, Sr (a) and Zr, Rb, Sr (b). The inventory numbers of the objects and the area analyzed (color, mark, glaze) are indicated (see Table 1).

Five groups are identifiable in the Y-Rb-Sr diagram (Figure 5): two groups on the Y-Sr line, the first corresponding to blue glazed areas (Group 1_Y), the second to half of the gildings (Group 2_Y); a group very close to the Rb-Sr line associating the base marks, glaze and some gilding (Group 3_Y); and, finally, two other groups, one in the center of the diagram corresponding to the other blue zones (Group 4_Y) and, below, a last group (Group 5_Y) mainly bringing together the purple zones and remaining gildings. The diagram with zirconium is not very discriminating, except for a distribution on a line going from the Rb peak to a Zr/Sr ratio close to 50% and the absence of Rb for part of the gildings. This comparison confirms the efficiency of the classifying character of the Y-Rb-Sr ternary diagram.

3.3. Blue Zones and Elements Associated with Cobalt

Cobalt ion was the main coloring agent of blue glass and enamels until the 1960s. Cobalt is a rare transition metal and a previous review has shown that geological sites could be classified into three groups [30]: (i) primary sites issued from metallic nodules of the deep ocean floor, formed by oxyhydroxides of all transition metals (Fe, Mn, Co, Ni, etc.) in many Asian mining places; (ii) the veins resulting from the dissolution of the primary sites and the precipitation of five elements (Ag, Bi, Co, Ni and Cu) in the form of arsenides and sulfides [30,52] at European sites in the Hercynian mountains; and (iii) salt lake evaporites from ultimate dissolution, as for some ancient Egyptian glass [30].

Figure 6 compares the ternary diagrams of the signals of the Ag-Cu-Bi and Ni-Zn-As elements. Previous studies (see reference [30] and references therein) have pointed out that these elements discriminate the origin of cobalt ores. Let us recall that the analyses of the

blue decorations of the very first porcelains of the 17th century show a significant signal of copper in association with that of cobalt [30,39] and cobalt was initially a by-product of the exploitation of silver (*zaffre* obtained from residual slag and then converted into *smalt* by mixing with potash glass) [30,53–55]. Then, cobalt is also a by-product of bismuth mining. However, it is difficult to know the precise relationship between the date of production and the levels of silver or bismuth. For the 16th and 17th centuries, it is assumed that, when the production of cobalt is a by-product of the productions of silver and bismuth, the detection of large traces of these elements is in agreement with this type of mine. Two groups are identifiable from the Ag-Cu-Bi ternary diagram of Figure 6a: the ones that are ‘rich’ in silver (the visualization mode based on the comparison of the signals exacerbates the differences and classifies them as relatively ‘rich’ compositions whose contents remain low) and without bismuth and the ones with bismuth. We believe that this corresponds to different mines. The Schneeberg mine (Saxony), exploited since the early Middle-Ages, is known to also produce bismuth [56]. On the other hand, the neighboring Freiberg mine also produced silver and cobalt but with zinc and uranium [57–60]. Indeed, Figure S2 (Supplementary Information) shows that the uranium signal defines different groups that may correspond to the above-mentioned mining places: Group 1_{U-As} being rich in uranium traces—likely the Freiberg mine—and Group 2_{U-As} being almost free of uranium, which may correspond to the Schneeberg mine.

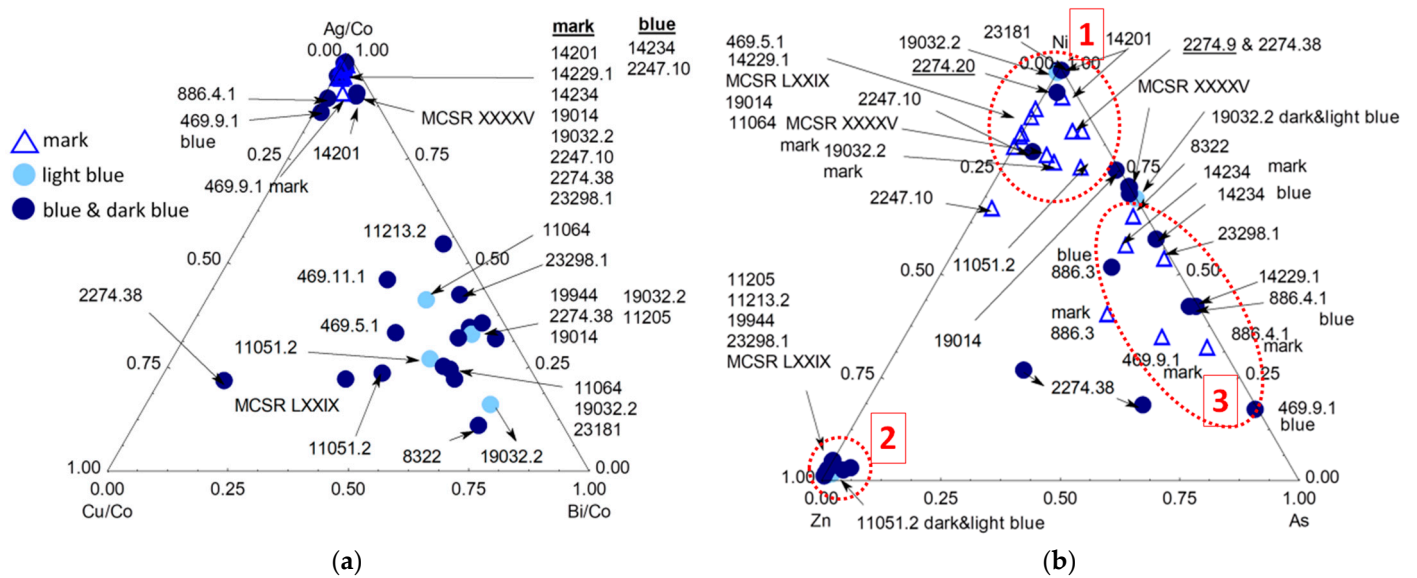









Figure 6. Comparison of the relative intensities of the signal of (a) the elements Ag, Cu and Bi (normalized by the signal of Co), Ni, Zn and As in the blue zones (mark and decorations) and (b) Sn, Zn and As (Groups 1 to 3 are discussed throughout the text).

Most of the marks belong to the ‘silver-rich’ or silver-containing group. Note the special behavior of gilded areas that also contain U, Ag and As traces. However, the added contribution of the substrate and flux is certain due to the thinness of the gold layer.

The Ni-Zn-As diagram (Figure 6b) shows three groups, one ‘rich’ in nickel (Group 1_{Ni-Zn}), the second ‘rich’ in zinc (Group 2_{Ni-Zn}; previous studies associated a high level of Zn with 19th century production [28]) and the third containing arsenic (Group 3_{Ni-Zn}, Table 3). Half of the marks only contain arsenic.

Table 3. Classification and validation of the date of production (no: no gilding or not measured) (photos by P. Colombar). The different groups (1, 2, etc.) identified according to different criteria (for the Raman signature of the glaze, the elements associated with the cobalt of the marks and/or blue decorations, the impurities of the glaze and gilding) are listed.

Inventory Number (Type)	Period	View	Glaze	Co and X Blue	Co and X Marks	CoBiPb Blue, Glaze and Marks	YRbSr	Au ^o	Classification
MNC 2274.20 (butter cup)	c.a. 1730		1	4	no	2,3	4	no	
MNC 2274.9 (2274.2) (bowl)	1726 (mark)		1	no	1	2	4	2	
MNC 19014 (coffee cup with arm coat of France and Poland)	1737 Gift from August III to Marie Leszcynska		1	4	1	1,2	4	2	
MNC 469.9.1 (coffee cup with painting copy)	ca. 1774–1814 (Marcolini period)		1	4	1	2,3	4	1	
MNC 886.4.1 (coffee cup)	End of 18th—beginning of 19th c.		1	4	1	2,3	4	1	
MNC 14234 (orange cup)	18th c.?		1	4	2	2,3	4	no	
MCSR XXXXV (Imari-style dish)	ca. 1730		1	4	2	2,3	4	1	

A Group

Table 3. Cont.








Inventory Number (Type)	Period	View	Glaze	Co and X Blue	Co and X Marks	CoBiPb Blue, Glaze and Marks	YRbSr	Au ^o	Classification
MNC 469.5.1 (coffee cup)	?		1	1,4	1	1,2	2	2	
MNC 19032.2 (mustard cup)	18th c.		1	4	2	1,2	2	no	B Group
MNC 469.11.1 (tea cup)	ca. 19th c.		1	1	no	1	2	2	
MNC 11064 (Group of three child geometers and astronomers)	18th c.?		no	1	1	1,2	1	2	
MNC 19944 (Singing angel)	18th c.			1	1		1	1	C Group
MNC 11213.2 (coffee cup)	18th c.		1	2	no	1,2	4	2	D
MNC 14201 (tea pot)	18th c.		1	3	5		4	1	E

Table 3. Cont.






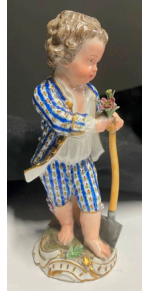





Inventory Number (Type)	Period	View	Glaze	Co and X Blue	Co and X Marks	CoBiPb Blue, Glaze and Marks	YRbSr	Au ^o	Classification
MCSR LXXIX (Chinese decoration)	ca. 1720–1730		1	6	2	1,2	2	2	F
MNC 2274.38 (Figure)	1709–1730		no	5	1	1,2	2	no	G
MNC 886.3	1825		3	4	3	2,3	4	no	H
MNC 2247.10			3	3	1	2,3	4	no	
MNC 23298.1 (cup for Turkish market)	ca. 1774		4	1	4	1,2	1	2	I
MNC 11051.2 (boy figure)	18th c.?		5	1	1	2	1,2	no	J

Table 3. Cont.

Inventory Number (Type)	Period	View	Glaze	Co and X Blue	Co and X Marks	CoBiPb Blue, Glaze and Marks	YRbSr	Au ^o	Classification
MNC 11205 (Bacchus and bacchante group)	18th c.		no	no	no	no	no	2	K
MNC 8160.2 (dish)	ca. 1720		no	no	no	no	no	no	
MNC 25340 (figure)	19th c.		no	no	no	no	no	no	Not studied using XRF
MNC 9638 (bowl)	18th c.		no	no	no	no	no	no	
MCSR LVII.1 (coffee cup with Watteau-like décor)	ca. 1745		no	no	no	no	no	no	

The observation of a fairly well-defined data cluster leads us to hierarchically classify the data concerning the signals of cobalt and associated elements (Figure 7). The hierarchical classification for all of the non-colored areas (glaze, Figure 7a) using elements associated with cobalt shows great homogeneity (most data belong to one group) except for the MNC 11051.2 figurine (Group 5_{Ag-Zn}) and, to a lesser extent, the MNC 23298.1 (Group 4_{Ag-Zn}) (tureen for Turkish market), MNC 886.3 (large dish) and MNC 2247.10 (large dish) artifacts (Group 3_{Ag-Zn}). These last two objects, purchased in 1825, were probably produced on that date. Artifact MNC 14229.1, the chocolate pot with a Chinese-style mark, is specific (Group 2_{Ag-Zn}) and its blue decoration contains arsenic.

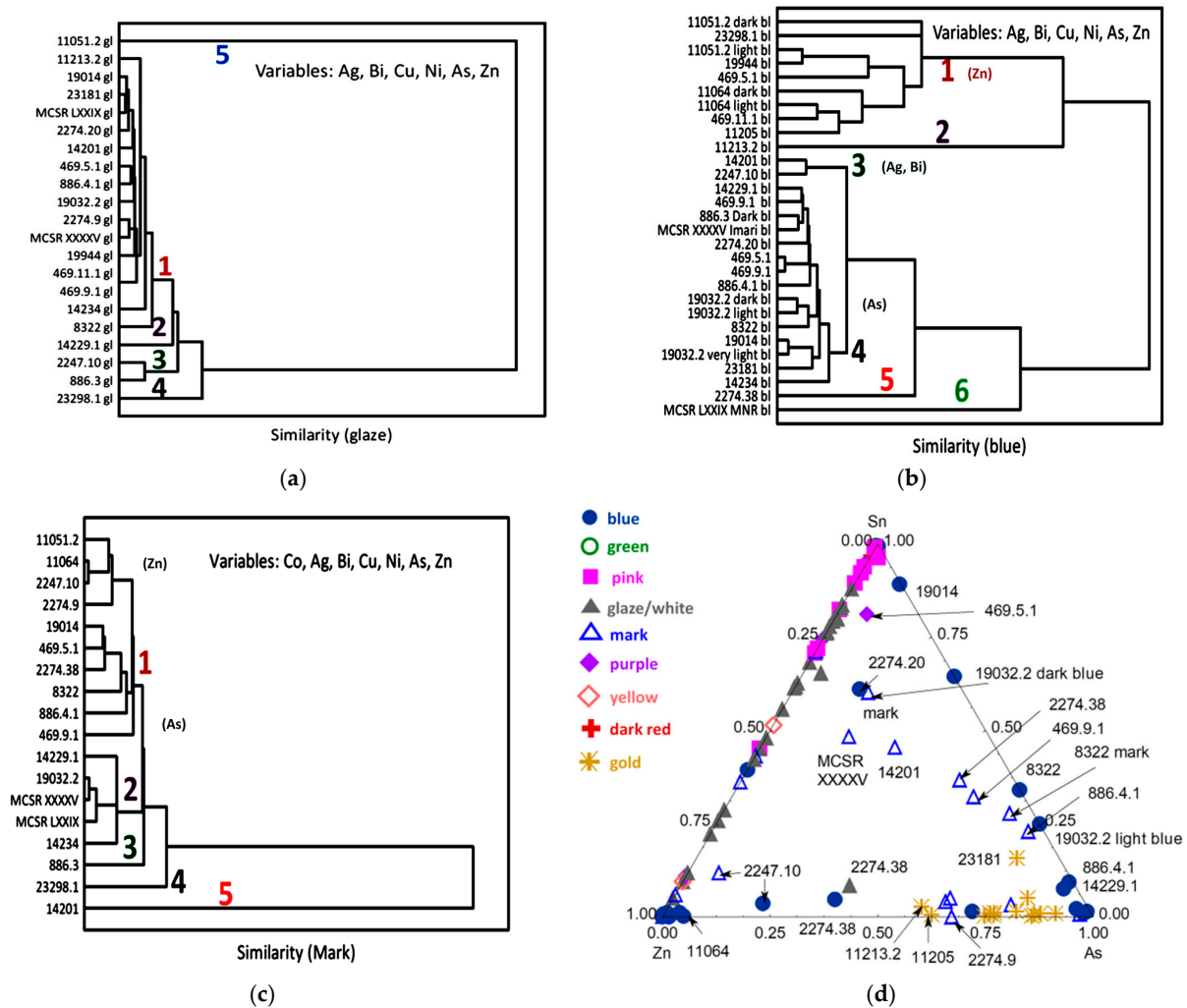


Figure 7. Diagrams of hierarchical similarity constructed with the variables indicated for the colorless glaze (a), blue areas (b) and the marks; (c) Sn-Zn-As signal diagram for all areas (d).

This great homogeneity of the classification related to the glaze (Figure 7a, most of them belong to Group 1_{Ag-Zn}) makes it possible to examine the classification carried out for the blue zones and the blue marks, the modification (‘pollution’) of the pXRF signal by the composition of the glaze covering the mark (underglaze mark), or located under the blue overglaze decoration, being similar and considered as constant. Thus, for the marks (Figure 7c), we obtain three groups (called Group “1”, “2” and “3”) with little differentiation apart from a few artifacts (called Group “4” and “5”), respectively, the MNC 23198.1 (Turkish market) and the MNC 14201 mark (tea pot with country decoration and gilding). Are these marks from the 18th century or later?

An examination of the diagram of all the blue zones (marks included, Figure 7b) according to the variables Ag, Bi, Cu, Ni, As and Zn shows two supergroups (“1 + 2” and “3 + 4”), those containing zinc (group 1 + 2, assigned to 19th century according to reference [28]) and those containing arsenic (3 + 4), plus one (MNC11051.2) and two objects (MNC 2274.38 (a figurine) and MCSR LXXIX (tureen with Chinese decoration)) being at the margins. Additional similarity diagrams using all variables, or specifically the Y/Sr/Rb, Pb/Ca/K/Ba and Sn/Zn/As groups, also detect particularities (Figure S3, Supplementary Materials).

In conclusion, the variability measured for the mark is weak, likely due to the strong contribution of the glaze and substrate that moderates the contribution of cobalt. We distinguish, however, As-free (Group 1, Figure 6b) and As-containing cobalt (Groupe 3). The

classification from the decoration measurement is efficient (Figure 7c) with the identification of two supergroups, blue with zinc (1 + 2) and with only arsenic (3 + 4).

The Raman spectra obtained on the blue areas do not show any characteristic signature of a particular pigment (spinel, cobalt aluminate or cobalt/olivine silicate [30]), which indicates that the Co^{2+} ions are perfectly dissolved in the amorphous silicate network. Indeed, up to middle of the 19th century, the coloration of silicate glass was obtained without the use of pigment, with cobalt ions being dissolved in the silicate network [30]. However, an intense mode characteristic of the As-O bond around 820 cm^{-1} is observed, e.g., for the objects MNC 2274.38, MNC 19032.2, MNC 11213.2, MNC 11064 and MNC 9638 (see Figure S1, Supplementary Materials for Raman spectra). This is typical when cobalt ore rich in arsenic is used to color a lead-rich glaze [30,38,43].

3.4. Other Colors: Green, Yellow, Red to Purple

The pink-to-purple color presents the Raman spectra characteristic of the presence of metallic nanoparticles, i.e., a broad fluorescence background (as for MNC 23181 (pink areas in Figure 3)). The diagrams of the relative intensities of the characteristic peaks of the elements Sn, Zn and As (Figure 7d) and Sn, Au and As (Figure 8b) show significant levels of tin in pink areas. This indicates that gold nanoparticles have been prepared using the Kunckel' method, also called Cassius' purple [61,62], and not using the Perrot method based on the reduction of soluble gold ions with arsenic [63,64]. The latter route is observed for many Qing Dynasty enameled porcelains, according to their relationship with French recipes [25,26].

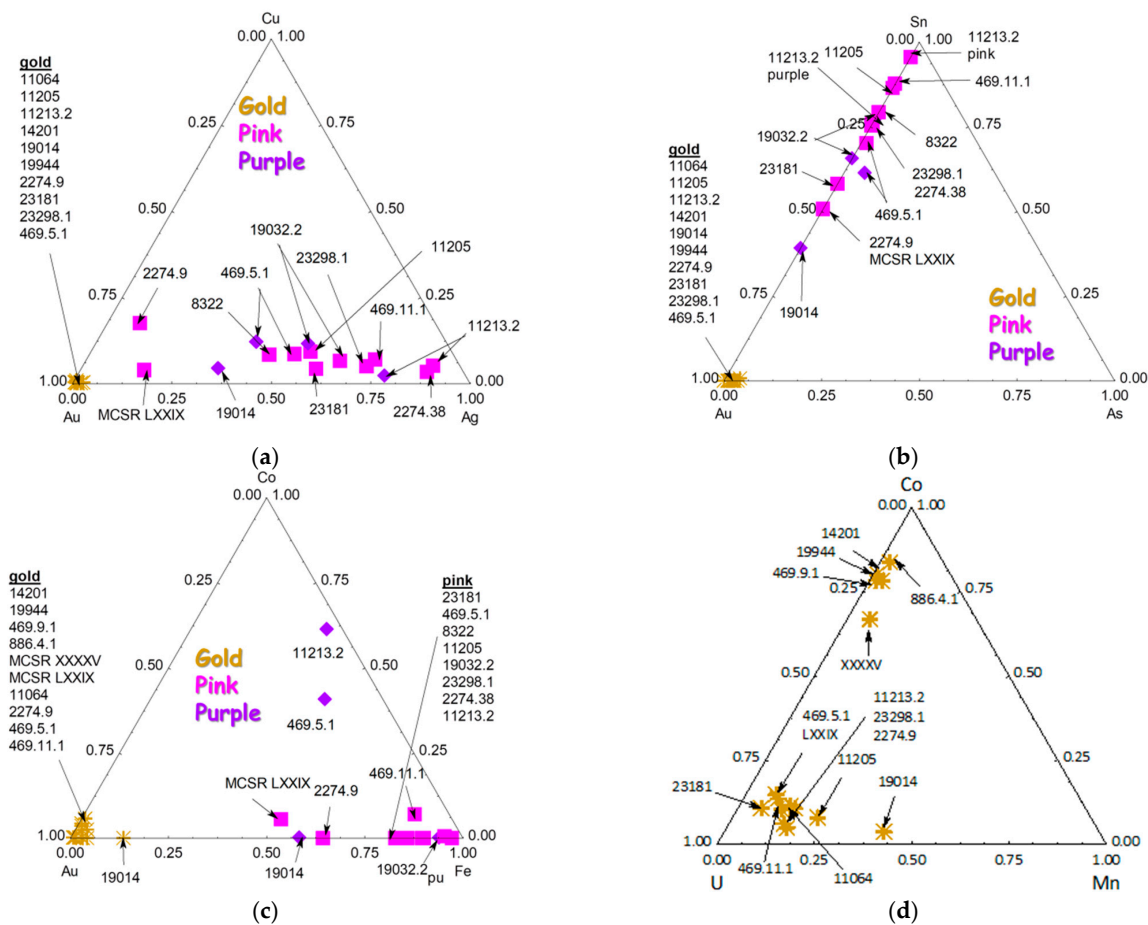


Figure 8. Cont.

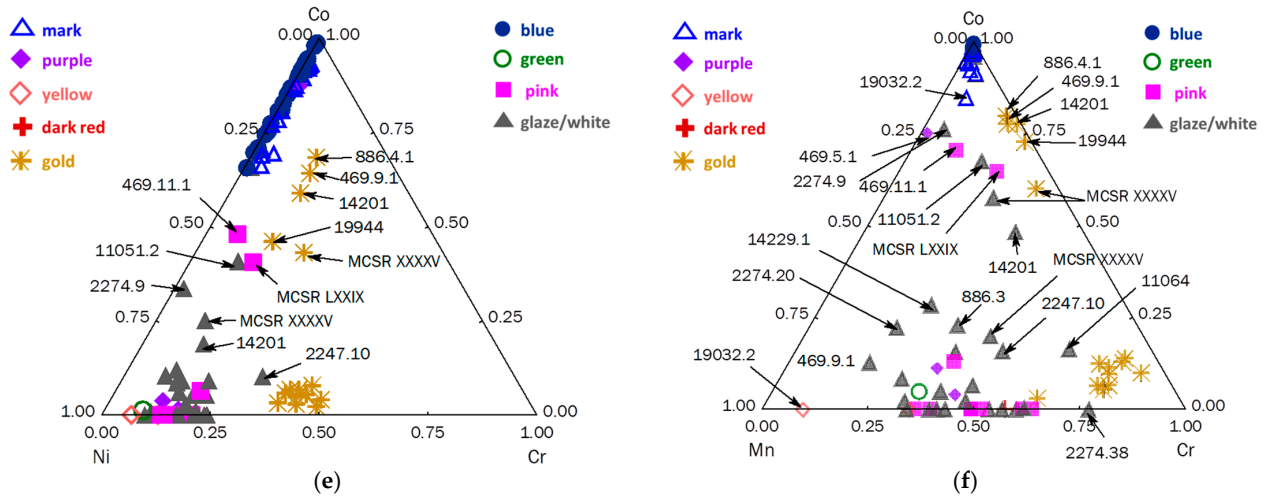


Figure 8. Comparison of the relative intensity of the characteristics peak of the Cu-Au-Ag (a), Sn-Au-As, (b), Co-Au-Fe (c), Co-U-Mn (d), Co-Ni-Cr (e) and Co-Mn-Cr (f) element signal diagrams for colored areas.

The overglazes that contain tin show the characteristic Raman doublet (635–775 cm^{-1} , e.g., MNC 19014, Figure 9); this is observed in the blue, yellow or green decorations of some objects (MNC 19032.2 and MNC 11205, Figure S1). Some purples are clearly obtained by adding cobalt (MNC 11213.2 and MNC 469.5.1) to pink recipes.

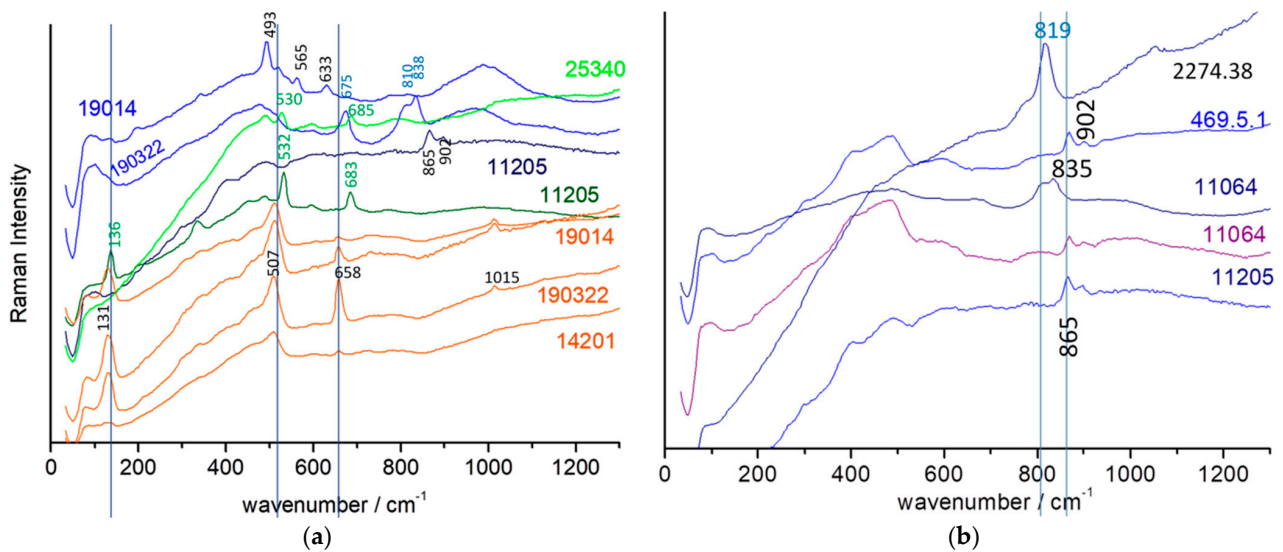


Figure 9. Comparison of representative Raman spectra recorded on blue (blue line), green/light green (green and light-green line) and yellow (orange line) areas of MNC 2530, MNC 11205, MNC 19014, MNC 190322, MNC 14201 (a) and MNC 2274.38, MNC 469.5.1, MNC 11064 and MNC 11205 artifacts (violet line: light blue area); (b) zoom of the 0-1300 cm^{-1} spectral range Lines are a guide for the eye.

3.5. Gilding

While the gold used for the gilding seems very pure (with no significant amount of silver, as is usually observed for many cases [50]), the gold used for the nanoparticles giving the pink to purple colors contains silver (Figure 8a), as observed for gilding made by Parpette or Coteau, both contemporary famous French enamellers [64].

The comparison of the signals of the Co and U elements recorded on gildings (Figure S2) shows two types of gilding, one with traces of uranium (Group 2_{Au}^o, MNC

11213, MNC 11205, MNC 19014, MNC 2274.9, MNC 11064, MNC 23181, MNC 23298.1, MNC 469.5.1, MNC 469.11.1 and MCSR LXXIX), and the second with traces of cobalt (Group 1 $_{Au^p}$, MNC 469.9.1, MNC 886.4.1, MNC 14201, MNC 19944 and MCSR XXXXV) (Figures 6 and 8). These two groups are identified in the Co-U-Mn (Figure 8d) and Co-U-As, Co-U-Ag, Co-Mn-Cr and Co-Ni-Cr diagrams (Supplementary Materials). It is assumed that the different impurities are characteristic of a different provenance/mining of gold (at least two different sources). The traces of uranium in the gold are always very weak and, therefore, the uranium observed by pXRF in the golden zones or colored by gold nanoparticles cannot come from the gold itself but either from a phase associated with the gold or from ingredients added for firing, in particular for the flux allowing adhesion (the addition of bismuth?).

A comparison of the Raman signatures measured on the areas colored in blue (light blue to dark blue), in green and yellow-green and in yellow shows an unexpected variety (Figures 9 and S1). Some signatures are fairly well documented, such as cassiterite (doublet at $633\text{--}775\text{ cm}^{-1}$) [10,31], lead-antimony pyrochlore pigment (doublet $131\text{--}507\text{ cm}^{-1}$) and its homologous lead-tin ($135\text{--}340\text{ cm}^{-1}$) [45–49] and lead calcium/potassium arsenate apatite ($\sim 820\text{ cm}^{-1}$) [30]. The presence of a band above 830 cm^{-1} in the blue glaze has been attributed to impurities containing chromium [30] according to pXRF data (Figure 8f).

Precise elementary analyses of the points showing these Raman signatures are necessary to attribute these vibrational signatures associated with chrome. It is possible that this could allow the establishment of groups indicating the use of the same raw materials.

4. Comparison with Earlier Böttger Production

The previously studied *boccaro* wares can be considered the first hard porcelains produced in Europe, although these objects are often called stoneware [1–4,6,7,65,66]. Polished artifacts show a very high level of densification [5] according to the qualification of porcelain. Indeed, the first kaolin identified by Böttger and von Tschirnhaus, coming mainly from Zwickau, was rich in iron and led to a red paste [1]. Alabaster was used as a flux, replaced in 1733 by feldspar [1,3,67–70], the common source of flux for continental European hard-paste porcelain [3–5,71–73]. Our previous work on French and Chinese porcelain glazes [24,25] demonstrated that the pXRF signals of impurities such as Y, Rb and Sr (rubidium is an impurity of sodium and potassium, strontium of calcium and yttrium of quartz) effectively classified the productions at the scales of the large geological contexts of the raw materials used for the different glazes. A comparison of the relative signals Y, Zr, Rb, and Sr of the objects of this study (Figure 10) with the previous data [6,7] concerning the red pastes of the Böttger stoneware and of 20th century replicas shows a small shift within the Y-Rb-Sr diagram, which agrees with the use of almost similar raw materials, regardless of the time elapsed between the two periods of production (both the data close to those recorded on the mark and on neighboring ‘white’ areas).

However, the Zr-Rb-Sr ternary (Figure 9b) shows a specific difference, with the *boccaro* wares being richer in zirconium, likely due to the use of a particular sand and/or the replacement of alabaster with feldspar after the death of Böttger and/or or a less refined cleaning/washing of raw materials. A comparison with modern productions (first half of the 20th century) also shows a shift due to the evolution of raw materials. This may offer some criteria to identify modern productions made using an ancient mold. The Pb-Ca-K (Figure 10c) and Ba-Ca-K (Figure 10d) ternaries show few differences, the Böttger data being close to those obtained in the present study for the marks and the contribution of the body being significant. Of course, larger differences are observed with data related to blue and polychrome glazes. Gold decorations appear to contain more barium, indicating the addition of a component with this impurity to the flux used for gilding.

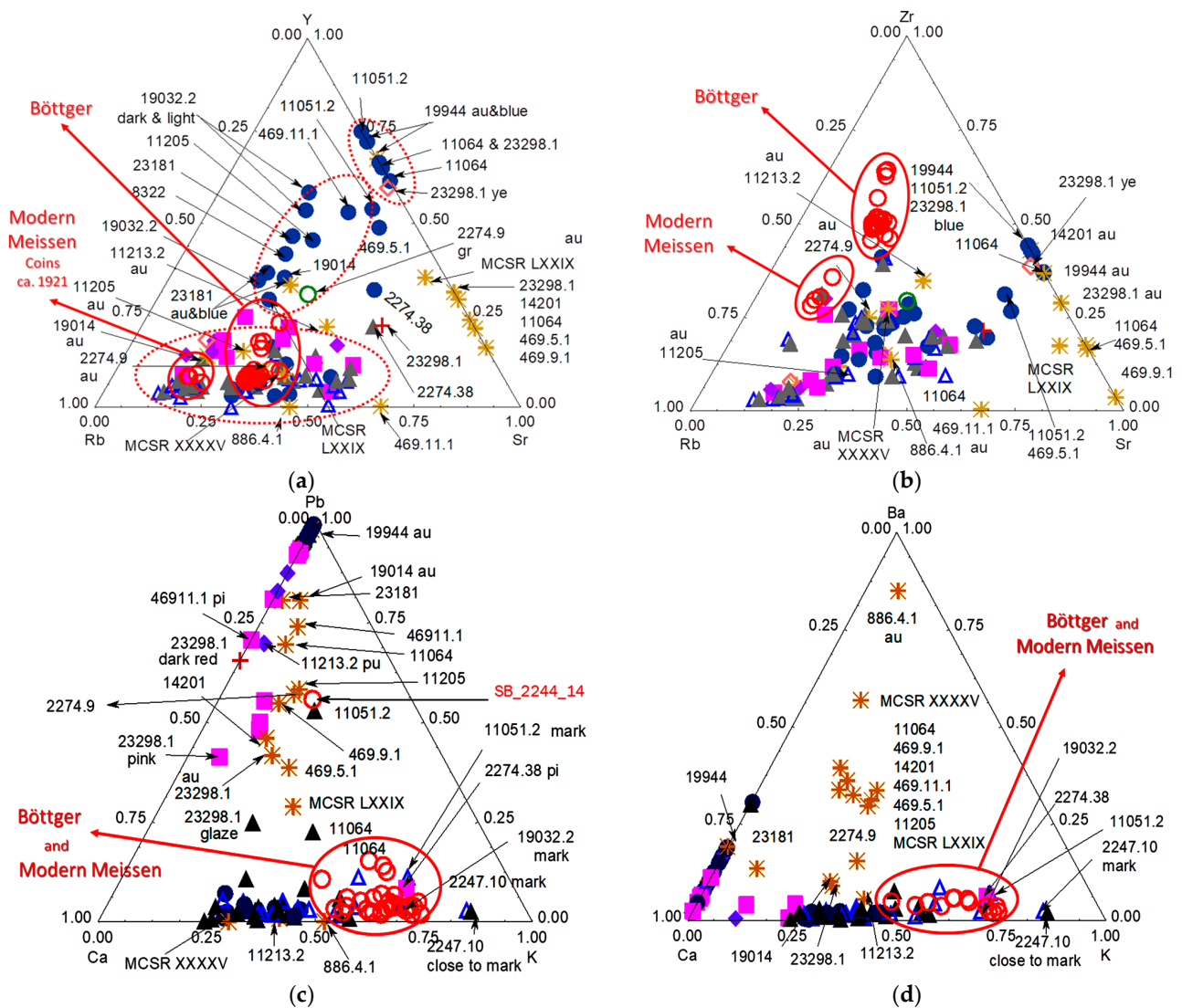


Figure 10. Comparison of the present data relative to Y-Rb-Sr (a), Zr-Rb-Sr (b), Pb-Ca-K (c) and Ba-Ca-K (d) signal with those previously recorded for red Böttger paste (*boccario* ware, red open circle; see previous figures for the explanation of other labels) references [6,7].

5. Tentative Dating and Discussion of Authentication Criteria

The first objective was to identify, through the resemblance/dissimilarity of the signatures of the composition (minor elements and traces) of the marks, the colored zones and the silicate matrices for the objects whose glazes and marks were expected to have been made with the same natural raw materials (and could be from the same period of production). Moreover, given the context of the processing of raw materials (there was little chemical treatment of ores during the 17th and 18th centuries [30,53,54]), objects produced during the same period should form clusters on ternary and hierarchical classification diagrams. Several parameters must be taken into account, including the following:

- (i) The first is the heterogeneity of the areas analyzed. Although the enamels are made of glass and a part is prepared using prior fusion, the heterogeneity should be important because of the raw materials' variability with time (the composition of rock shifts with its location in many quarries) and the decoration's realization. Also, we will use the elements associated with the coloring elements but that give a visible signal pXRF.
- (ii) The second is that, during the period considered, the 18th and 19th centuries, the processing of ores, for example, cobalt, evolved considerably and, therefore, the

residual content of the associated elements evolved too [30]. Furthermore, different qualities (e.g., grades of *smalt*) may have been reported [74].

We present in Table 3 several classifications using different criteria:

- (i) The first concerns the silicate matrix constituting the glaze (Raman data);
- (ii) The second considers the elements associated with cobalt in the blue areas;
- (iii) The third, the elements detected in the mark;
- (iv) The fourth, those—cobalt included—detected in all the blues (*décor* and marks);
- (v) Those according to the groups identified in the Y-Rb-Sr ternary diagram;
- (vi) And, additionally, the characterization of gilded areas.

The combination of these different classification criteria leads to the identification of the “homogeneous” groups listed in Table 3. We will classify the artifacts as Group X, for which most of the classification criteria are identical. Group A comprises seven objects, Group B has three pieces and then two Groups are associated with two artifacts (Group C and Group H). For the other seven objects, differences concerning the criteria do not make it possible to associate them in a clear way. Thus, the first conclusion of this work is that, with the exception of objects produced during the first half of the 18th century, productions were carried out by combining raw materials from different origins in a variable manner. On the other hand, the base marks show less heterogeneity. The variability of the ingredients used to make the body appears low.

Group A contains objects whose decoration and/or marks, but also historical information, allow dating after ca. 1725–1730 (post Böttger period) but before the middle of the 18th century. Unexpectedly, two cups with characteristic end-of-18th-century—early 19th century decoration (the ‘Marcolini’ period) belong to this group, which indicates continuity in the use of raw materials for certain objects, likely those for quality customers. For two objects (MNC 14234 orange cup with swords and K-mark and MCSR XXXXV Imari-style plate with black mark), the cobalt of the marks calls into question the authenticity of these marks.

Group B corresponds to three cups with a sophisticated polychrome decoration. For these objects, the Y-Rb-Sr criterion associated with the silicate matrix of the enamel is different, no doubt due to the firing constraints of the polychrome decoration. One artifact (MNC 469.11.1 cup) shows very characteristic 19th century decoration. As for the two 19th century cups of Group A (MNC 469.9.1 and MNC 886.4.1), it is obvious that these artifacts were made with the same raw materials as those used in the 18th century for the production of sophisticated pieces. One can conclude that specific raw materials were used specifically for high-quality objects during these decades.

A few remarks can be made for the other objects. The two dishes purchased in 1825 (MNC 886.3 and MNC 2247.10) are very similar in decoration but differ in the impurities associated with the marks. The MNC 2274.38 figurine does have a mark like Group A—its model is given from 1709 to 1730 in the old catalogue—but, in terms of the other criteria, it deviates from Group A. We can assume that the polychromatic decoration was posed and fired in the 19th century on a biscuit fired before. The MNC 23298.1 bowl with a famous decoration intended for the Ottoman Empire market has a specific glaze and mark (Table 1).

The two groups based on traces associated to gilded areas do not correspond to other groups; however, it seems that Group 1_{Au} (with Co) corresponds more to older productions than Group 2_{Au} (with U). The uranium level must be confirmed using a more precise (but destructive) method on the shards.

6. Did Chinese Enamellers Use Parisian or Saxon Recipes?

Previous works comparing Chinese and French porcelains showed that the Chinese enamels from Qing Dynasty data fell into three groups:

- (i) Those made using imported raw materials, mainly from the Paris region, were rich in traces of yttrium, located at the top on the Y-Sr line;
- (ii) Those based on Chinese raw materials on the Rb-Sr line (i.e., without Y) are located on the side rich in Rb (as for Yuan and Ming Dynasty production);

(iii) Those located on the line parallel to Y-Rb were obtained by mixing Chinese and imported ingredients.

Table 4 summarizes the specific information related to the composition and phases in Qing Dynasty overglazes as a function of the recipes, both the traditional ones used during the Ming Dynasty or new ones imported from Europe.

Table 4. Main composition and phase characteristics of Qing Dynasty overglaze.

Color	Coloring Agent Colorant/Opacifiant	Element(s) Associated with Coloring Agent/Phase(s)	Glassy Silicate Matrix/ Associated Elements	Recipes/ Ingredients Origin	Reference
White	Different types of lead arsenates		Y	Europe	[24,25,51]
	cassiterite			Europe	[22,23,26]
Blue	Co ²⁺	As/lead arsenate Ni,Cu	Y	Europe	[22–26,30,38,40,51]
	Co ²⁺	Fe,Mn	Rb,Sr	China	[24–26,30,38,40]
Yellow	Pb-Sn pigment			China/ Japan	
	Pb-Sb pyrochlore		Y	Europe	[22–26,30,38,51]
	Pb-Sb/Sn/Zn pyrochlore		Y	Europe	
Yellow-green	Co ²⁺ + yellow pigment		Y	Europe	
Green	Co ²⁺ + yellow pigment	As	Y	Europe	[22–24,26,38,43]
	Cu ²⁺			Europe/ China	
Red	Hematite			Europe/ China	[22,23,26,38,43]
	Cu ⁰ NPs			Europe/ China	[26,51]
	Au ⁰ NPs	As/lead arsenate	Y	Europe	[24–26,43,51]
Orange	Au ⁰ NPs			Europe	[24–26,43,51]
Rose/pink	Au ⁰ NPs	As/lead arsenate	Y	Europe	[24–26,43,51]
Purple	Au ⁰ NPs			Europe	
Black	Fe-Mn spinel			Europe/ China	[22–26,30,38,51]
	Fe-Mn-Cr spinel			Europe/ China	
Brown	Mn oxide			Europe/ China	

Let us recall that the importation of ingredients from Europe is attested both by the correspondence of the Jesuits [28] and the Qing archives of the Imperial City [17–21].

A comparison with the data obtained on the productions of Meissen both confirms the previous conclusions but also moderates them. Four groups are identifiable: the group of measurements concerning the marks where the kaolin-based mullite paste and the glaze contribute strongly to the signals is located, as for the Chinese porcelains, near the Rb-Sr line. On the other hand, a certain number of blue decorations are similar to the production of French soft-paste porcelain, which is rich in yttrium traces. Some blue decorations are located on the line parallel to the Y-Rb line, a criterion indicating a distribution between end-members. As reported in Table 4, yttrium traces appear to be characteristic of the

European ingredients. If this cannot correspond to a mixture of European and Chinese cobalt—we are considering Meissen porcelain—, this indicates the use of different cobalt, as the diagrams using the signals of uranium, silver and bismuth prove. This opens up the possibility that certain raw materials were imported to China from Germany via the connections of the German Jesuit K. Slumpf. Consequently, the assignment of the use of a mixture of imported French and local Chinese ingredients should be changed to the use of imported Meissen ingredients (or their mixture with Chinese ones). The number of objects prepared using raw materials originating from Europe should be larger than in our previous conclusions. The Y-Rb-Sr diagram is not effective in differentiating the marks due to the contribution of the paste substrate or even that of the glaze. It is essential to consider the elements associated with cobalt (Figure 8) in order to check the presence of Fe and Mn characteristic of Asian ores.

7. Conclusions

This analysis of a series of objects from Sèvres museum, which are categorized as representative of 18th and 19th century Meissen productions, shows both variability and permanencies concerning the use of raw materials recognizable by the minor elements or traces associated with the silicate matrix of the glazes and the cobalt used in the mark or the decoration. The natural raw materials come from quarries where the composition and assembly of rock are variable. This is why, today, this intrinsic variability is averaged by mixing many clays, kaolin and feldspar/pegmatite to obtain a product with an almost stable average composition and constant rheological/plasticity properties, as well as dilatometric/sintering behavior. This variability means that the analytical criteria obtained through elemental analysis must be compared with those obtained using other techniques, such as the identification of the phases (pigments, opacifiers) which depend not only on the raw materials but also on the firing process and the information obtained from stylistic analysis (the model that defined or influenced the decor, color palette and touch specific to an enamel painter) or historical information (document, text, engraving, etc.).

The combination of several classification criteria concerning the type of glaze, the elements associated with cobalt in the mark or the blue decor and the relative levels of impurities characteristic of the raw materials and giving a strong XRF signal leads to the identification of four groups of homogeneous objects (respectively, seven, three, two and two objects), the other seven objects presenting too many differences to be considered as having been produced with the same raw materials (seven other artifacts have been only analyzed using Raman microscopy). The first group brings together almost all the objects with a reliable pedigree, but includes two objects with decoration types from ~1800 period. The three objects in the second group are characterized by polychromatic decoration. For some artifacts, the gap between the conclusions made on the mark and the decoration leads us to suppose that an enamel decoration was placed on biscuits produced several years earlier. Obviously, cobalt was being sourced from different mining places, likely from Saxony but also likely from other places. Valmont de Bomare reports that many grades of *smalt* were available in Paris by 1774 [75] and this was likely the same at the Meissen factory.

If we compare this study to similar studies carried out on Iznik production [75], the variability of pXRF or Raman data is much higher at the Meissen factory than that of Ottoman production (16th–17th centuries), which was carefully controlled by the Ottoman services (*nakkashane*). A similar remark can be made for Safavid crockery production, which shows low variability [32]. The dispersion of the characteristic data also appears greater than those measured on Qing imperial productions made with Chinese raw materials [24,25]. We might think that the development of production at Meissen at the end of the 18th century and during the 19th century led to diversification in production quality/cost, requiring the use of various raw materials. This information on the diversity of raw materials would have to be compared with administrative information and on the quantities produced to reconstruct the industrial and economic dynamics of the factory. It would be interesting to compare this information with the productions of other

large contemporary factories such as those of Sèvres, Strasburg, Capo di Monte, Tournai, Saint-Petersburg, etc.

If some blue glazes show the characteristic Raman signature of lead arsenate with an apatite structure commonly observed in the painted overglazes of French and Chinese porcelains [24,25,32], the other Raman signatures observed do not show this signature, which agrees with the use of ‘purified’ cobalt or of cobalt coming from sources other than Saxony, in agreement with the mention reported by d’Albis and Magetti about the use at Sèvres of cobalt from the Pyrenees Mountains [11]. The common assumption of considering the Erzgebirge (Johanngeorgenstadt, Annaberg, Schneeberg, Marienberg, Freiberg and Joachimsthal,) as the single source of cobalt for blue decoration of European pottery should probably be reviewed and efforts must be made to find information in the archives relative to other European mining places: Schwarzwald, Thuringia and Harz, in Germany, Sainte-Marie-aux-Mines in France, etc., most of them having been active since almost the Middle-Ages. [30,31] This difference in Raman signature between the Meissen productions and, on the other hand, the French and Chinese productions reinforces arguments for attributing the French Jesuits as having a determining influence on the transfer of enameling technology to the craftsmen of the Qing court.

The comparison of the signals of the impurities of the raw materials or the minor elements associated with cobalt reinforces the possibility of identifying the use of ingredients and, in particular, of cobalt imported from Europe for the production of the painted enamels of the Qing dynasty. However, some of the glazes attributed to the use of a mixture of Chinese ingredients and those used in France may, in fact, also correspond to those used in Meissen (Figure 11d). A more complete analysis on the basis of rare elements will provide additional information. This work shows both the potential and the limitation of non-invasive analyses carried out on site, which limit the measurement to the close ‘skin’ of objects. The impossibility of focusing pXRF on the richest area of the coloring agent—as possible on a (polished) section of a shard under a microscope or with an ion beam—makes it impossible to avoid the contribution of the surrounding material, which makes it more difficult to extract relevant information. It is not possible to identify all the elements and their isotopes as allowed by LA-ICP-MS, micro-destructive analysis. However, the post-processing approaches presented in this work allowed us to access significant details that can contribute to elucidating not only the production techniques but also the origin of the objects studied.

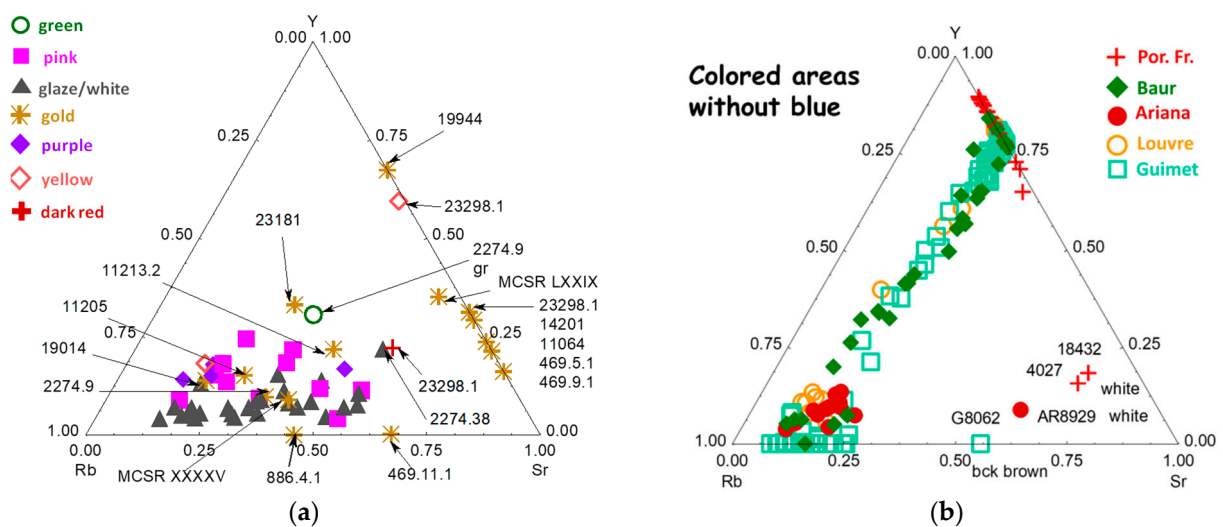


Figure 11. Cont.

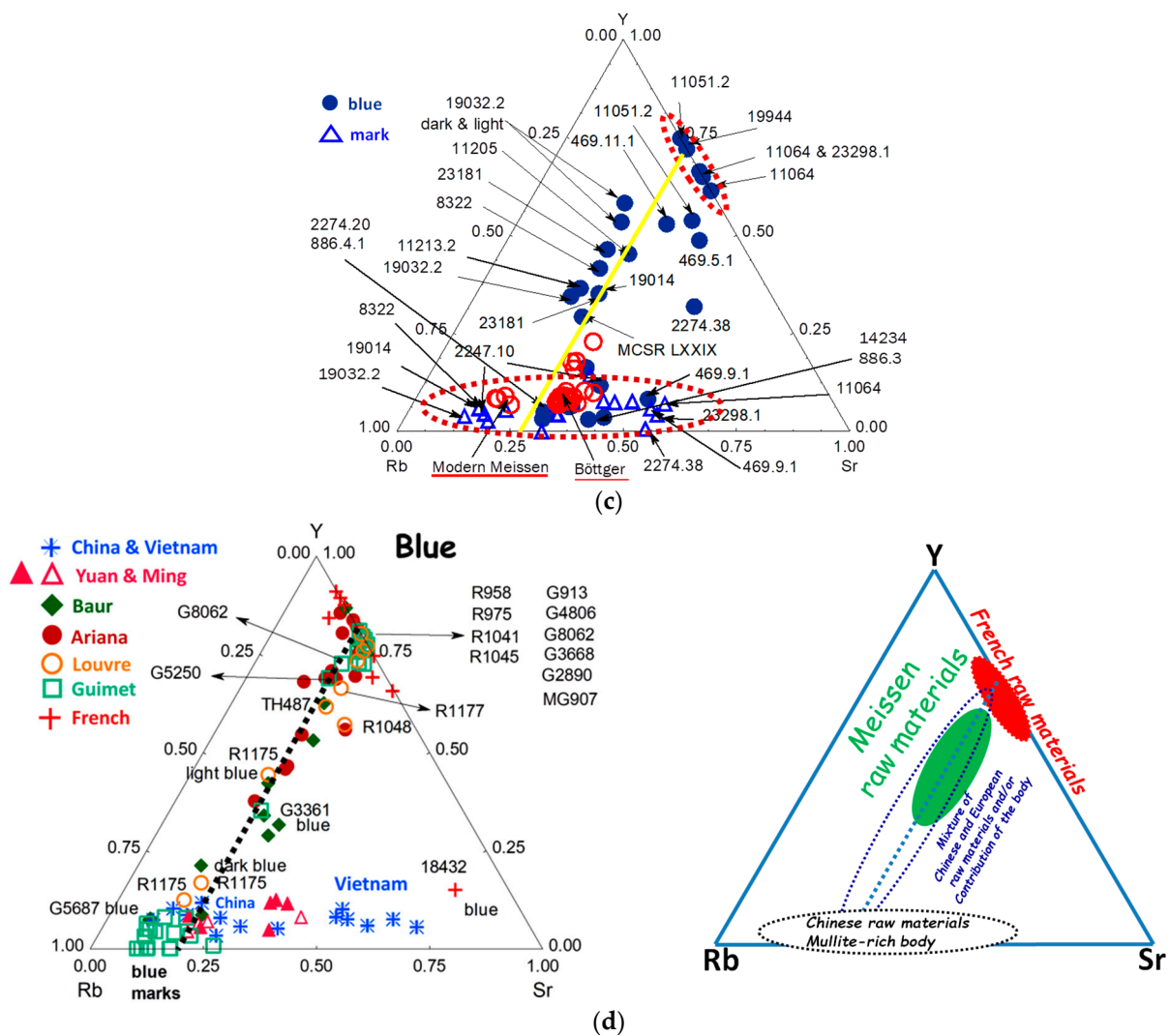


Figure 11. Comparison of pXRF signals relative to Y, Rb and Sr content for Meissen (a,c) and for Qing Chinese porcelain glazes from the 18th century (b,d); collections of the museums of Paris (Musée des Arts Asiatiques-Guimet and Musée du Louvre) and Geneva (Musée de l’Ariana and Musée de la Fondation Baur) and French porcelain glazes from the end of the 17th and beginning of the 18th century (Por. Fr., Collection Cité de la Céramique, Sèvres) (c,d) according to data from references [26,51]. For comparison, data on blue-and-white porcelains from the earlier Yuan and Ming dynasties (including Vietnamese productions) are also indicated. Blue areas: (c,d); other colors: (a,b). (d) Graphical conclusion.

Supplementary Materials: The following supporting information can be downloaded at: <https://www.mdpi.com/article/10.3390/ceramics6040134/s1>: Table S1: Analyzed artifacts: date of production and acquisition; Figure S1: As-recorded Raman and pXRF spectra of artifacts. Figure S2: Comparison of the relative intensities of the signal of the elements Co, U and Ag in the different areas; Figure S3: Diagrams of hierarchical similarity constructed with all the variables—or those indicated for areas indicated.

Author Contributions: Conceptualization, P.C.; methodology, P.C., G.S.F., M.G. (Mareike Gerken) and M.G. (Michele Gironda); investigation, P.C. and M.G. (Michele Gironda); resources, P.C. and V.M.; writing—original draft preparation, P.C. and G.S.F.; writing—review and editing, P.C., G.S.F., M.G. (Mareike Gerken), M.G. (Michele Gironda) and V.M. All authors have read and agreed to the published version of the manuscript.

Funding: The work was partially funded by the French Agence Nationale de la Recherche Enamel FC project ANR-19-CE27-0019-02.

Data Availability Statement: Data are given in the Supplementary Materials.

Conflicts of Interest: Authors Mareike Gerken and Michele Gironda were employed by the company Bruker Nano Analytics. The authors declare that the research was conducted in the absence of any commercial or financial relationships that could be construed as a potential conflict of interest.

References

1. Goder, W.; Schulle, W.; Wagenbreth, O.; Walter, H. *Meissen, La Découverte de la Porcelaine Européenne en Saxe—J.F. Böttger; Pigmalion-Gérard Watelet*; Paris, France, 1984.
2. von Hornig Sutter, M. Meissener Porzellane des 18. Jahrhunderts im Visier von Kunstgeschichte und Naturwissenschaft. *Weltkunst* **1985**, *55*, 110–115.
3. Kingery, W.D. The development of European porcelain. In *High-Technology Ceramics: Past, Present, and Future—The Nature of Innovation and Change in Ceramic Technology; Technology and Style, Ceramic and Civilization Series*; Kingery, W.D., Ed.; The American Ceramic Society: Westerville, OH, USA, 1986; Volume III, pp. 153–180.
4. d’Albis, A. The history of innovation in European porcelain manufacture and the evolution of style: Are they related? In *Technology and Style, Ceramic and Civilization*; Kingery, W.D., Ed.; The American Ceramic Society: Westerville, OH, USA, 1986; Volume III, pp. 397–412.
5. Colomban, P.; Milande, V. On-site Raman analysis of the earliest known Meissen porcelain and stoneware. *J. Raman Spectrosc.* **2006**, *37*, 606–613. [[CrossRef](#)]
6. Simsek, G.; Casadio, F.; Colomban, P.; Bellot-Gurlet, L.; Faber, K.T.; Zelleke, G.; Milande, V.; Moinet, E. On-site Identification of Early Böttger Red Stoneware made at Meissen using portable XRF: 1, Body Analysis. *J. Am. Ceram. Soc.* **2014**, *97*, 2745–2754. [[CrossRef](#)]
7. Simsek, G.; Casadio, F.; Colomban, P.; Bellot-Gurlet, L.; Faber, K.T.; Zelleke, G.; Milande, V.; Moinet, E. On-site Identification of Early Böttger Red Stoneware made at Meissen using portable XRF: 2, Glaze and Gilding Analysis. *J. Am. Ceram. Soc.* **2015**, *98*, 3006–3013. [[CrossRef](#)]
8. d’Albis, A. Steps in the Manufacture of the soft-paste porcelain of Vincennes, According to the book of Hellot. In *Ceramic and Civilization I: Ancient Technology to Modern Science*; Kingery, W., Ed.; The American Ceramic Society: Columbus, OH, USA, 1985; pp. 257–272.
9. Colomban, P.; Treppoz, F. Identification and Differentiation of Ancient and Modern European Porcelains by Raman Macro- and Microspectroscopy. *J. Raman Spectrosc.* **2001**, *32*, 93–102. [[CrossRef](#)]
10. Colomban, P.; Robert, I.; Roche, C.; Sagon, G.; Milande, V. Identification des porcelaines “tendres” du 18^{ème} siècle par spectroscopie Raman: Saint-Cloud, Chantilly, Mennecey et Vincennes/Sèvres. *Rev. D’archéométrie* **2004**, *28*, 153–167. [[CrossRef](#)]
11. Maggetti, M.; d’Albis, A. Phase and compositional analysis of a Sèvres soft paste porcelain plate from 1781, with a review of early porcelain techniques. *Eur. J. Mineral* **2017**, *29*, 347–367. [[CrossRef](#)]
12. Demirsar Arli, B.; Simsek Franci, G.; Kaya, S.; Arli, H.; Colomban, P. Portable X-ray Fluorescence (p-XRF) Uncertainty Estimation for Glazed Ceramic Analysis: Case of Iznik Tiles. *Heritage* **2020**, *3*, 1302–1329. [[CrossRef](#)]
13. Colomban, P.; Milande, V.; Lucas, H. On-site Raman analysis of Medici porcelain. *J. Raman Spectrosc.* **2004**, *35*, 68–72. [[CrossRef](#)]
14. Deron, I.; Colomban, P. Le trafic maritime de la Compagnie des Indes. *manuscript in preparation*.
15. *Père d’Entrecolle’s Letters from Ching-te-chen in 1712 and 1722, Translated in R. Tichane, Ching-te-Chen*; New York State Institute for Glaze Research, Painted Post: New York, NY, USA, 1983.
16. Finlay, J. *Henri Bertin and the Representation of China in Eighteenth-Century France*; Routledge: New York, NY, USA, 2020.
17. Shih, C.-f. Evidence of East-West Exchange in the Eighteenth Century: The Establishment of Painted Enamel Art at the Qing Court in the Reign of Emperor Kangxi. *Natl. Palace Mus. Res. Q.* **2007**, *24*, 45–94.
18. Curtis, E.B. Aspects of a multi-faceted process: The circulation of enamel wares between the Vatican and Kangxi’s court. *Extrême-Orient Extrême-Occident.* **2019**, *43*, 29–39. [[CrossRef](#)]
19. Shih, C.-F. Hua Falang: The Chinese Concept of Painted Enamels. In *The RA Collection of Chinese Ceramics: A Collector’s Vision*; Jorge Welsh Research & Publishing: London, UK, 2021; Volume V, pp. 28–59.
20. Shih, C.-f. L’Avènement d’une nouvelle palette de couleurs à Jingdezhen au XVIII^e siècle. In *Le Secret des Couleurs. Céramiques de Chine et d’Europe du XVIII^e Siècle à Nos Jours*; d’Abrigeon, P., Ed.; 5 Continents Editions & Fondation Baur: Milan, France, 2022; pp. 21–59.
21. Bellemare, J. A New Palette: Reassessing the Development of Enamel Colors in Early-Eighteenth-Century China. *J. Glass Stud.* **2022**, *64*, 147–167. Available online: <https://www.jstor.org/stable/48703407> (accessed on 30 September 2023).
22. Colomban, P.; Zhang, Y.; Zhao, B. Non-invasive Raman analyses of huafalang and related porcelain wares. Searching for evidence for innovative pigment technologies. *Ceram. Inter.* **2017**, *43*, 12079–12088. [[CrossRef](#)]
23. Colomban, P.; Gironda, M.; Vangu, D.; Kırmızı, B.; Zhao, B.; Cochet, V. The technology transfer from Europe to China in the 17th–18th centuries: Non-invasive on-site XRF and Raman analyses of Chinese Qing Dynasty enameled masterpieces made using European ingredients/recipes. *Materials* **2021**, *14*, 7434. [[CrossRef](#)] [[PubMed](#)]

24. Colomban, P.; Simsek Franci, G.; Gironde, M.; d'Abrigeon, P.; Schuhmacher, A.-C. pXRF Data Evaluation Methodology for On-Site Analysis of Precious Artifacts: Cobalt Used in the Blue Decoration of Qing Dynasty Overglazed Porcelain Enamelled at Customs District (Guangzhou), Jingdezhen and Zaobanchu (Beijing) Workshops. *Heritage* **2022**, *5*, 1752–1778. [[CrossRef](#)]
25. Colomban, P.; Simsek Franci, G.; Burlot, J.; Gallet, X.; Zhao, B.; Clais, J.B. Non-Invasive on-Site pXRF Analysis of Coloring Agents, Marks and Enamels of Qing Imperial and Non-Imperial Porcelain. *Ceramics* **2023**, *6*, 447–474. [[CrossRef](#)]
26. Colomban, P. Tracer l'utilisation de recettes et/ou d'ingrédients européens dans les objets émaillés: Stratégie et premiers résultats. *Artefact* **2023**, *18*, 161–193. [[CrossRef](#)]
27. Landry-Deron, I. La contribution des missionnaires aux arts du feu à la cour de Pékin (XVII^e–XVIII^e siècles). *Artefact* **2023**, *18*, 117–137. [[CrossRef](#)]
28. Klisinska Kopacz, A.; Wilkosz, T.; Ochniak Dudek, K. X-ray Analysis of Eighteenth- and Nineteenth-Century Meissen Porcelain Figurines. *J. Anthr. Archaeol. Sci.* **2023**, *7*, 964–974.
29. Domoney, K.; Shortland, A.J.; Kuhn, S. Characterization of 18th-century Meissen porcelain using SEM-EDS. *Archaeometry* **2012**, *54*, 454–474. [[CrossRef](#)]
30. Colomban, P.; Kirmizi, B.; Simsek Franci, G. Cobalt and associated impurities in blue (and green) glass, glaze and enamel: Relationships between raw materials, processing, composition, phases and international trade. *Minerals* **2021**, *11*, 633. [[CrossRef](#)]
31. Colomban, P.; Simsek Franci, G. Timurid, Ottoman, Safavid and Qajar Ceramics: Raman and Composition Classification of the Different Types of Glaze and Pigments. *Minerals* **2023**, *13*, 977. [[CrossRef](#)]
32. Fiches d'inventaire du Musée national de Céramique, 6 Grande Rue, 92310, Sèvres, France (This database can be consulted on request on site at the Cité de la Céramique).
33. Pannequin, B.; Préaud, T.; Bezut, K.; d'Albis, A.; Dahlberg, L.; Lajoix, A.; Millasseau, S. *The Sèvres Porcelain Manufactory: Alexandre Brongniart and the Triumph of Art and Industry, 1800–1847*; Yale University Press: New Haven, CT, USA, 1997.
34. Fourest, P.-H. *Porcelaine de Saxe, Exhibition Catalog, 4th July–1st September 1952, Musée national de Céramique, Sèvres*; Editions des musées nationaux: Paris, France, 1952.
35. Pietsch, U. *Triumph of the Blue Swords: Meissen Porcelain for Aristocracy and Bourgeoisie 1710–1815*; Exhibition Cat., 8th May–25th August 2010; Dresdner Porzellansammlung, Zwinger: Dresden, Germany, 2010.
36. Mission D'étude sur la Spoliation des Juifs de France, 1998–2000. Available online: <https://www.culture.gouv.fr/Nous-connaitre/Organisation-du-ministere/Le-secretariat-general/Mission-de-recherche-et-de-restitution-des-biens-culturels-spolies-entre-1933-et-1945/Biens-Musees-Nationaux-Recuperation-MNR> (accessed on 21 September 2023).
37. Available online: <https://xrfcheck.bruker.com/InfoDepth> (accessed on 6 July 2022).
38. Colomban, P.; Ambrosi, F.; Ngo, A.-T.; Lu, T.-A.; Feng, X.-L.; Chen, S.; Choi, C.-L. Comparative analysis of *wucaï* Chinese porcelains using mobile and fixed Raman microspectrometers. *Ceram. Inter.* **2017**, *43*, 14244–14256. [[CrossRef](#)]
39. Colomban, P.; Gironde, M.; Edwards, H.G.M.; Mesqui, V. The enamels of the first (softpaste) European blue-and-white porcelains: Rouen, Saint-Cloud and Paris factories: Complementarity of Raman and X-ray fluorescence analyses with mobile instruments to identify the cobalt ore. *J. Raman Spectrosc.* **2021**, *52*, 2246–2261. [[CrossRef](#)]
40. Burlot, J.; Gallet, X.; Simsek Franci, G.; Bellot-Gurlet, L.; Colomban, P. Non-Invasive On-site pXRF Analysis of Coloring Agents, Marks and Glazes: Variability and Representativity of Measurements on Qing porcelain. *Colorants* **2023**, *2*, 42–57. [[CrossRef](#)]
41. Colomban, P. Polymerisation Degree and Raman Identification of Ancient Glasses used for Jewellery, Ceramics Enamels and Mosaics. *J. Non-Crystall. Solids* **2003**, *323*, 180–187. [[CrossRef](#)]
42. Colomban, P.; Tournié, A.; Bellot-Gurlet, L. Raman Identification of glassy silicates used in ceramic, glass and jewelry: A tentative differentiation guide. *J. Raman Spectrosc.* **2006**, *37*, 841–852. [[CrossRef](#)]
43. Colomban, P.; Ngo, A.-T.; Fournery, N. Non-invasive Raman Analysis of 18th Century Chinese Export/Armorial Overglazed Porcelain: Identification of the Different Enameling Technology. *Heritage* **2022**, *5*, 233–259. [[CrossRef](#)]
44. Edwards, H.G.M.; Vandenabeele, P.; Colomban, P. *Raman Spectroscopy in Cultural Heritage Preservation*; Springer: Cham, Switzerland, 2022.
45. Colomban, P.; Sagon, G.; Faurel, X. Differentiation of antique ceramics from the Raman spectra of their coloured glazes and paintings. *J. Raman Spectrosc.* **2001**, *32*, 351–360. [[CrossRef](#)]
46. Sakellariou, K.; Miliiani, C.; Morresi, A.; Ombelli, M. Spectroscopic investigation of yellow majolica glazes. *J. Raman Spectrosc.* **2004**, *35*, 61–67. [[CrossRef](#)]
47. Sandalinas, C.; Ruiz-Moreno, S.; Lopez-Gil, A.; Miralles, J. Experimental confirmation by Raman spectroscopy of a Pb-Sn-Sb triple oxide yellow pigment in sixteenth-century Italian pottery. *J. Raman Spectrosc.* **2006**, *37*, 1146–1153. [[CrossRef](#)]
48. Rosi, F.; Manuali, V.; Miliiani, C.; Brunetti, B.G.; Sgamellotti, A.; Grygar, T.; Hradil, D. Raman scattering features of lead pyroantimonate compounds. Part I: XRD and Raman characterization of Pb₂Sb₂O₇ doped with tin and zinc. *J. Raman Spectrosc.* **2009**, *40*, 107–111. [[CrossRef](#)]
49. Pelosi, C.; Agresti, G.; Santamaria, U.; Mattei, E. Artificial yellow pigments: Production and characterization through spectroscopic methods of analysis. *E-Preserv. Sci.* **2010**, *7*, 108–115. Available online: <http://www.morana-rtd.com/e-preservationscience/2010/Pelosi-10-05-2010.pdf> (accessed on 25 May 2023).
50. Colomban, P.; Calligaro, T.; Vibert-Guigue, C.; Nguyen, Q.L.; Edwards, H.G.M. Dorures des céramiques et tesselles anciennes: Technologies et accrochage. *ArchéoSciences* **2005**, *29*, 7–20. [[CrossRef](#)]

51. Colomban, P.; Girona, M.; Simsek Franci, G.; d'Abrigeon, P. Distinguishing Genuine Imperial Qing Dynasty Porcelain from Ancient Replicas by On-site Noninvasive XRF and Raman Spectroscopy. *Materials* **2022**, *15*, 5147. [[CrossRef](#)] [[PubMed](#)]
52. Kissin, S.A. Five Elements (Ni-Co-As-Ag-Bi) Veins, Geoscience Canada 19[3] (1992). pp. 113–124. Available online: <https://journals.lib.unb.ca/index.php/gc/article/view/3768/4282> (accessed on 15 December 2019).
53. Delamare, F. Aux origines des bleus de cobalt: Les débuts de la fabrication du saffre et du smalt en Europe occidentale. *Comptes Rendus Séances L'académie Inscr. Belles-Lett.* **2009**, *153*, 297–315. [[CrossRef](#)]
54. Delamare, F. Saffre, smalt, bleu d'esmail et azur. In *Bleus en Poudres, 5 000 ans D'innovations Techniques*; Prese des Mines: Paris, France, 2008.
55. Zlamalova Cilova, Z.; Gelnar, M.; Randakova, S. Smalt production in the ore mountains: Characterization of samples related to the production of blue pigment in Bohemia. *Archaeometry* **2020**, *62*, 1202–1215. [[CrossRef](#)]
56. Available online: <https://www.mindat.org/locentry-627563.html> (accessed on 1 August 2023).
57. Gratuze, B.; Soulier, I.; Barrandon, J.N.; Foy, D. De L'origine du Cobalt Dans les Verres. *Rev. D'archéométrie* **1992**, *16*, 97–108. Available online: https://www.persee.fr/doc/arsci_0399-1237_1992_num_16_1_895 (accessed on 30 September 2023). [[CrossRef](#)]
58. Gratuze, B.; Soulier, I.; Blet, M.; Vallauri, L. De L'origine du Cobalt: Du Verre à la Céramique. *Rev. D'archéométrie* **1996**, *20*, 77–94. Available online: https://www.persee.fr/doc/arsci_0399-1237_1992_num_16_1_939 (accessed on 30 September 2023). [[CrossRef](#)]
59. Wesch, H.; Wiethage, T.; Spiethoff, A.; Wegener, K.; Müller, K.M.; Mehlhorn, J. German uranium miner study: Historical background and available histopathological material. *Radiat. Res.* **1999**, *152*, S48–S51. [[CrossRef](#)]
60. Scheinert, M.; Kupsch, H.; Bletz, B. Geochemical investigations of slags from the historical smelting in Freiberg, Erzgebirge (Germany). *Geochemistry* **2009**, *69*, 81–90. [[CrossRef](#)]
61. Hunt, L.B. The true story of Purple of Cassius. *Gold Bull.* **1976**, *9*, 134–139. [[CrossRef](#)]
62. Geyssant, J.; Gorget, C.; Tétart-Vittu, F. *Bernard Perrot (1640–1709), Secrets et Chefs-D'œuvre des Verreries Royales D'orleans*; Exhibition Catalogue, Musée des Beaux-Arts d'Orléans—SOMOGY Editions d'Arts: Paris, France, 2013.
63. Colomban, P.; Kirmizi, B. Non-invasive on-site Raman study of white and polychrome enamelled glass artefacts in imitation of porcelain assigned to Bernard Perrot and his followers. *J. Raman Spectrosc.* **2020**, *51*, 133–146. [[CrossRef](#)]
64. Colomban, P.; Kirmizi, B.; Clais, J.-B. Coteau' jewelled porcelain: A summit of ceramic art. On-site Raman and pXRF study. *J. Eur. Ceram. Soc.* **2020**, *40*, 4664–4675. [[CrossRef](#)]
65. Swann, C.P.; Nelson, C.H. Böttger stoneware from North America and Europe: Are they authentic? *Nucl. Instr. Meth. Phys. Res. B* **2000**, *161–163*, 694–698. [[CrossRef](#)]
66. Simsek Franci, G.; Colomban, P. On-Site Identification of Pottery with pXRF: An Example of European and Chinese Red Stonewares. *Heritage* **2022**, *5*, 88–102. [[CrossRef](#)]
67. Ullrich, B.; Lange, P.; Friedmar, K. Thüringer und Meissener Porcellan des spatter 18. und frühen 19. Jahrhunderts-ein werkstoffhistorischer Vergleich. *Keram. Zeitsch.* **2010**, *62*, 185–190.
68. Casadio, F.; Bezur, A.; Domoney, K.; Eremin, K.; Lee, L.; Mass, J.L. X-ray fluorescence applied to overglaze enamel decoration on eighteenth- and nineteenth-century porcelain from central Europe. *Stud. Conserv.* **2012**, *57*, S61–S72. [[CrossRef](#)]
69. Neelmeijer, C.; Pietsch, U.; Ulbricht, H. Eighteenth-century Meissen porcelain reference data obtained by proton-beam analysis (PIXE-PIGE). *Archaeometry* **2014**, *56*, 527–540. [[CrossRef](#)]
70. Schulle, W.; Goder, F.W. Die Erfindung des europäischen Porzellans durch Böttger—Eine systematische schöpferische Entwicklung. *Keram. Ztschr.* **1982**, *34*, 598–600.
71. Edwards, H.G.M. *Porcelain Analysis and Its Role in the Forensic Attribution of Ceramic Specimens*; Springer: Cham, Switzerland, 2022.
72. Edwards, H.G.M. *18th and 19th Century Porcelain Analysis in A Forensic Provenancing Assessment*; Springer: Cham, Switzerland, 2020. Available online: <https://www.springer.com/gp/book/9783030421915> (accessed on 15 December 2021).
73. Bezur, A.; Casadio, F. The Analysis of Porcelain Using Handheld and Portable X-ray Fluorescence Spectrometer. In *Studies in Archaeological Sciences: Handheld XRF for Art and Archaeology*; Shugar, A., Mass, J., Eds.; Leuven University Press: Leuven, Belgium, 2013.
74. Valmont de Bomare, M. *Minéralogie, ou Nouvelle Exposition du Règne Minéral*, 2nd ed.; Vincent Imprimeur-Libraire: Paris, France, 1774; pp. 76–96.
75. Colomban, P.; Milande, V.; Le Bihan, L. On-site Raman analysis of Iznik pottery glazes and pigments. *J. Raman Spectrosc.* **2004**, *35*, 527–535. [[CrossRef](#)]

Disclaimer/Publisher's Note: The statements, opinions and data contained in all publications are solely those of the individual author(s) and contributor(s) and not of MDPI and/or the editor(s). MDPI and/or the editor(s) disclaim responsibility for any injury to people or property resulting from any ideas, methods, instructions or products referred to in the content.